Forestry: An International Journal of Forest Research, 2026, 99(2), cpag022
https://doi.org/10.1093/forestry/cpag022
Published: 25 March 2026
Original Article

Towards a near real-time remote sensing monitoring system of forest canopy cover loss in Bavaria, Germany

Niklas Jaggy[1,*], Frank Thonfeld[2], Patrick Kacic[1], Nikolas Herbst[3], Mareike Kortmann[4], Samuel Kounev[3], Jörg Müller[4], Claudia Kuenzer[1,2]

[1]Department of Remote Sensing, Institute of Geography and Geology, University of Würzburg, John-Skilton-Str. 4a, D-97074 Würzburg, Germany
[2]German Remote Sensing Data Center (DFD), German Aerospace Center (DLR) Oberpfaffenhofen, D-82234 Wessling, Germany
[3]University of Würzburg, Chair of Software Engineering, Am Hubland, D-97074 Würzburg, Germany
[4]University of Würzburg, Chair of Conservation Biology and Forest Ecology, Ökologische Station Fabrikschleichach, Glashüttenstraße 5, 96181 Rauhenebrach, Germany

[*]Corresponding author. Department of Remote Sensing, Institute of Geography and Geology, University of Würzburg, John-Skilton-Str. 4a, D-97074 Würzburg, Germany.
E-mail: niklas.jaggy@uni-wuerzburg.de

Abstract

In the recent past, droughts and climate change-related impacts have led to declining vitality of forests in Central Europe. In combination with an increasing frequency of disturbances, this created a need for consistent large-scale monitoring of forest dynamics. Remote sensing and particularly new multispectral satellite missions now offer high-quality data streams that enable the development of new spatially continuous monitoring systems. However, current remote sensing-based operational forest monitoring systems typically suffer from either low spatial or temporal resolution and often also do not reach near real-time (NRT) capabilities. Here, we present a novel implementation of a forest monitoring system with high spatial and temporal resolution that is capable of providing NRT information on the state of forests for the entire federal state of Bavaria, Germany. Our monitoring system considers all relevant Sentinel-2 and Landsat-8/9 scenes since 2017 and utilizes the disturbance index to detect canopy cover loss on a biweekly basis for historic time series as well as in the form of NRT updates. For the latter, a computationally efficient data-driven method is implemented to detect disturbances for each new time step. An ancillary context layer is created to ensure robustness of NRT results. Our combined approach shows an overall accuracy of 0.85 with an F1 score of 0.81. Different spatial aggregation units reveal distinct hot spots of forest canopy cover loss across entire Bavaria with a total area of about 161 000 ha lost in a 7-year time period, including single districts losing over 20% of forest canopy cover. Our NRT component is able to contribute in closing the gap of timely information on canopy cover loss dynamics.

Keywords disturbance, time series, Earth observation, Sentinel, Landsat

Introduction

Recent years have seen a decline in forest condition of European forests, with a variety of environmental factors putting pressure on forest ecosystems (Buras *et al.* (2020), Senf *et al.* (2020), Rakovec *et al.* (2022), Thonfeld *et al.* (2022), Knapp *et al.* (2024), Lange *et al.* (2024)). Moreover, an increase in occurrence and severity of disturbances in European forests has been detected since the 1950s (Patacca *et al.*, 2022). The drivers of natural forest disturbances are manifold and create complex disturbance patterns. Particularly high impacts in recent years were caused by repeated drought years, which were linked to excess tree mortality across Europe (Senf *et al.*, 2020) and cascading effects (Brito, 2021) through higher susceptibility to both biotic and abiotic pressure, such as insect infestations or storm events. Consequently, assessments of forest condition revealed a general decline in forest vitality (Potocic *et al.*, 2021) that included large-scale stocked forest loss in both coniferous and deciduous forests (Haberstroh *et al.* (2022), Hartmann *et al.* (2022), West *et al.* (2022)) with Germany alone losing 501 000 ha of forest canopy cover between 2018 and 2021 (Thonfeld *et al.*, 2022). Additionally, the annual forest condition monitoring in Germany, which uses ground-based surveys since the 1980s, reported that in 2024 only 21% of tree crowns show no signs of defoliation (BMEL, 2025). These developments created a need for a consistent and coherent forest monitoring system (Patacca *et al.*, 2022) able to fill the lack of temporal and spatially continuous data on tree mortality (Hartmann *et al.*, 2022). Up-to-date assessments about the forest condition are important since the time and spatial distribution of forest disturbances affect the ecosystem services it provides (Thom and Seidl, 2015). In addition, continuous forest monitoring enables data-driven evaluations of forest management responses, which in turn

Handling Editor: Dr. Fabian Fassnacht
Received: 14 July 2025. **Revised:** 8 January 2026. **Accepted:** 26 January 2026

is important to inform policy-making processes toward sustainable forest management.

Satellite remote sensing is widely recognized as an efficient method to provide continuous data on the state of forests across large areas. It is therefore broadly applied for monitoring forest disturbances, attribution of disturbance drivers, and general assessments of the dynamic nature of forests across different spatial and temporal scales (Hermosilla *et al.* (2015), Wulder *et al.* (2020), Stahl *et al.* (2023)). Satellite image time series are used for monitoring long-term impacts as well as for observing short-term processes through recent image acquisitions. Especially the latter point is taken up more frequently in recent years and Senf *et al.* (2017) argued for a near-real time (NRT) monitoring in the context of insect disturbances, while others extend these thoughts to the level of NRT forest inventories (Coops *et al.*, 2022).

Compared with *in situ* forest monitoring, which is often spatially discontinuous with limited temporal resolution, NRT information from satellite observations provides distinct advantages for assessing forest ecosystem dynamics at high spatio-temporal resolution. Since a disturbance itself and the drivers behind it are complex in space and time, high temporal resolution data allow insights into the disturbance dynamics along the time dimension, which are not possible when monitoring forests e.g. in annual intervals. An NRT monitoring system makes timely implementations of management interventions feasible, which can be particularly relevant for some types of disturbances such as pests. NRT monitoring can also contribute to a deeper understanding of the changing dynamics of European disturbance regimes, as it is more suited to capture nuances of the spatio-temporal dynamics associated with the increased frequency of forest disturbances (Senf and Seidl 2021b). Finally, information derived from such NRT monitoring systems could also be integrated into forest planning activities by regularly updating existing field inventory data, which may be quickly outdated due to the observed increasing disturbance frequencies (Coops *et al.*, 2022).

Several advanced methods have been proposed for NRT detection of anomalies in satellite image time series. The S-CCD algorithm (Ye *et al.*, 2021) builds upon the CCDC approach (Zhu *et al.*, 2020) and extends it to an NRT monitoring method. It considers each new observation of a dense Landsat time series and recursively models the temporal dynamic. The Fordead approach (Dutrieux *et al.*, 2025) was developed in light of bark beetle infestations in French spruce forests. It includes a harmonic model that is fitted to a 2-year healthy period of a vegetation index, which serves as the basis of its predictions. New observations are compared with the model predictions with significant differences considered a signal for stress or disturbance events. Bfast Monitor (Verbesselt *et al.*, 2012), on the other hand, models the variation of a seasonal and trend signal in an automatically defined stable period in the past satellite image time series. This period serves as a reference for comparison with new observations for detecting anomalies if the observation crosses a probability boundary. However, all of these approaches require initial training of a statistical model or fitting a model to a defined stable period. This process requires careful parameter tuning to achieve accurate results. Additionally, all three algorithms come with certain scalability issues or at least require specific hardware when applying it to large areas. Although several NRT methods exist that leverage algorithms capable of handling multi-sensor input (BEAST: (Mulverhill *et al.*, 2023), TIIC: (Pelletier *et al.*, 2024), NRT-MONITOR: (Shang *et al.*, 2022)), neither is implemented over Europe. Furthermore, the resulting maps are typically only available at 30 m resolution, which do not cover the entire year (TIIC) or are not focused on forest disturbances (NRT-MONITOR).

Against the backdrop of the continuous vitality decline of German forests over the past decades (BMEL, 2025), several nation-wide remote sensing-based products have been developed to monitor forest condition using satellite data. These monitoring systems vary in input satellite data, selected indices, temporal and spatial resolution as well as update interval. For example, Buras *et al.* (2021) published a forest condition monitor (Waldzustandsmonitor,WZM) covering Germany and Europe that relies on postprocessed MODIS data. With a spatial resolution of > 200 m and data available as 8-day composites, it provides pixel- and date-specific Normalized Difference Vegetation Index (NDVI) quantiles and deviation from the median since 2001. A second forest condition monitor was proposed by Lange *et al.* (2024) and utilizes a forest condition anomaly (FCA) index. In this case, tree species-specific reference time series between 2016 and 2022 are taken to represent the reflectance variation. The FCA is then used as a similarity metric for new individual observations, aggregated into yearly, seasonal, and monthly FCA products at 20 m spatial resolution (UFZ-ForestConditionMonitor, UFZ (2024)). The Forest Monitor Germany (WaldmonitorDeutschland) provides information on vitality trends for German forests from 2016 to 2024. It uses Sentinel-2 data from May to September in monthly aggregates and compares maximum NDVI values across years to detect forest disturbances. In combination with normalized difference water index data, analyses across years allows the detection of trends in forest vitality and water balance (NWA & RSS, 2024). The approach of ForestWatch (LUP, 2024), on the other hand, relies on a vitality change percentage metric that uses Sentinel-2 data with low cloud probability. Monthly composites at 10 m spatial resolution of the disease water stress index (DWSI) from June to August are combined into a median composite, which is compared with a 2017 reference. The percentage deviations are subsequently aggregated in seven classes that allow comparisons of forest vitality annually from 2018 to 2023.

Although all of these products provide great information value on large geographical scale, each individual has its limitations. Whereas some are able to assess forest condition at high resolution (10 m), they only come with annual temporal resolution with the corresponding long update interval (Waldmonitor Deutschland). Others are able to process data both at denser time intervals of 8 days and for up to >20 years in the past, but only through the means of medium-resolution input data (WZM). A consistent observation across all products is that, although different sensor systems are used, each approach itself relied on single-sensor input data. Furthermore, none of the described products is currently implemented in the form of an operational NRT system that provides information without a significant delay in updates. At the European level, Mermoz *et al.* (2024) adopted an NRT tropical forest loss detection method based on Sentinel-1 data to monitor forest clear cuts in France at a sub-monthly interval, demonstrating how radar-based forest monitoring can be implemented for temperate forests. At the global level, several NRT products are available that feed data into early warning and alerting systems. However, the vast majority operate in or around tropical forests (Carter *et al.*, 2024). The proposed solutions differ notably in spatial resolution (10–50 m), sensor (optical vs. SAR), coverage (basin to global), and update interval (1–42 days). Whereas SAR methods are the preferred approach compared with optical methods over cloud-prone tropical regions (e.g. Reiche *et al.* (2021), Mullissa *et al.* (2024)), other global systems rely on optical data (Hansen *et al.*, 2016). Even a system

integrating different individual approaches exists (Reiche *et al.*, 2024). The latter also addresses the issue of robustness through multiple observations in continuous change detection algorithms (Coops *et al.*, 2022), by increasing confidence through each contributing alert over time. Results from methods primarily developed for deforestation detection in tropical forests that are later transferred or integrated in global alerting systems should be carefully evaluated before applying them in the temperate forests of Germany without ensuring the generalization capability of the methods in question. This is in large part due to the different characteristics of tropical and temperate forest disturbances. While in the tropics in most cases of human forest degradation the entire tree is removed (Bourgoin *et al.*, 2024), in Germany dead trees may remain in the forest as standing deadwood for extended time periods (Senf *et al.*, 2018).

In Germany, as well as on federal state level, there is currently only one operational forest monitoring product that provides NRT information on forest disturbances. The product is based on the method developed by Schiller *et al.* (2024) and available upon individual request via the EO-Lab platform. It provides Germany-wide model predictions of forest disturbances at a 5-day interval since June 2024 at 10 m spatial resolution based on Sentinel-2 data. The conversion to a binary classification and adding temporal information needs to be performed by the user. All other existing forest disturbance products have a temporal resolution of 1 month or longer, which do not consider winter observations, and provide unsatisfactory update intervals. In addition, none of the aforementioned products quantifies canopy cover losses, i.e. the stage at which trees are either dead or removed. The only data product providing canopy cover loss information in Germany at high spatial and temporal resolution (10 m, monthly) was developed by Thonfeld *et al.* (2022) and recently updated (Thonfeld *et al.*, 2026). However, the product is only updated upon request and does not set its focus on NRT processing. Sub-monthly forest disturbance alerts from global initiatives, on the other hand, suffer from the drawback that the algorithms are not tailored to temperate forests.

This work aims to close this gap by demonstrating how an operational system for high temporal and spatial resolution forest monitoring can be implemented for the entire German state of Bavaria. The objectives are to provide information at a biweekly interval at 10 m spatial resolution on the following:

1. forest disturbance date
2. disturbance magnitude

Additionally, we present the results of our past and NRT disturbance detection implementations. The resulting data products are made available to the public through an experimental mobile app to support forest management, decision-making processes, and policy making. We present our findings on both the development of the monitoring system and detected forest disturbances in Bavaria for the past 7 years.

Materials and methods

Study area

The methods in this study are applied to all forested areas in the entire federal state of Bavaria (Fig. 1). Forests cover 37% of the state area, amounting to 26 170 km^2, which is above the national average (4. Bundeswaldinventur/National Forest Inventory). The temperate forests stretch from mountainous alpine areas to hilly lowlands and are dominated by four tree species. These include primarily Norway spruce (*Picea abies*, 38.8%) and Scots pine (*Pinus sylvestris*, 16.8%), followed by European beech (*Fagus sylvatica*, 15.3%) and oaks (*Quercus petraea* and *Quercus robur*, 7.4%) (LWF, 2024). Spruce is the economically most important species, which makes up the majority of harvested wood (Statistisches Bundesamt (Destatis), 2024). It is often grown as as plantation forests in monocultures. The distribution of forest types follows an elevation gradient with coniferous trees dominating higher altitudes and deciduous species the lowlands, while midlands are characterized by mixed forests (Coleman *et al.*, 2024). Forest ownership is divided into private, communal, and state forests. With 56%, private forests constitute the largest share of ownership type, followed by state and communal ownership with 30% and 13%, respectively (LWF, 2024). Under these different ownership types, Bavarian forests experience a wide range of management practices, ranging from natural forests free of human intervention in the core zones of national parks to industrial wood production in the form of spruce monocultures. In recent years, Bavarian forests suffered from multiple stress factors, resulting in a continuous decrease of forest vitality. The forest condition survey (Waldzustandserhebung) by the Bavarian State Institute of Forestry (LWF) underlines how the drought years between 2018 and 2022 led to widespread damage to tree crowns (thinning) across tree species (LWF, 2023), fitting well into the overall trend of increasing natural forest disturbances (Senf *et al.*, 2018) and disturbance impact (Patacca *et al.*, 2022) in Europe. In Bavaria, disturbances occur at different scales and in diverse patterns (Reinosch *et al.*, 2024). Significant disturbances over the last years included large-scale windthrows and bark beetle infestations in spruce stands, insect infestations (*Thaumetopoea processionea*, *Lymantria dispar*) in oak trees, and beech stands suffering complex damages.

Datasets and preprocessing

Our study bases on earth observation (EO) and ancillary data. We applied EO data from the Sentinel-2 and Landsat-8/9 missions, both providing multispectral data at spatial resolutions between 10 and 60 m (Drusch *et al.* (2012), Roy *et al.* (2014)). While the Landsat missions go back several decades, Sentinel-2 data have been available since 2015. For this work, all scenes from both missions covering Bavaria from 2017 to present day with <80% cloud cover were selected (Fig. 2). For Sentinel-2, the Level-2A surface reflectance products processed by Sen2core (Pignatale, 2022) were considered with new scenes from the three satellite constellation provided at an ∼5-day revisit time, depending on latitude. Regarding the Landsat-8/9 constellation, we chose the Collection 2 data, which are surface reflectance values derived by the LaSRC algorithm (Crawford *et al.*, 2023). Combining Landsat-8 and Landsat-9 halves the nominal revisit time of 16 days. Due to the improved latency between image acquisition and availability of the processed data of 4–11 days and 2–3 days for Landsat 8 and 9 (Crawford *et al.*, 2023), respectively, the data are well suited for our NRT application. Together with the satellites from the Sentinel-2 mission, the combined revisit times can lead to observations on consecutive days or even double coverage on the same day. All data were provided in a data science storage container from the terrabyte high-performance data analysis platform and are therefore well integrated with its large high-performance computing resources necessary for processing multi-year time series at high spatial resolution (Terrabyte, 2024). The core of our approach follows the method developed by Thonfeld *et al.* (2022) with several alterations and extensions. This refers mainly to datasets for cloud masking that were unavailable to us and slight differences in the forest mask applied.

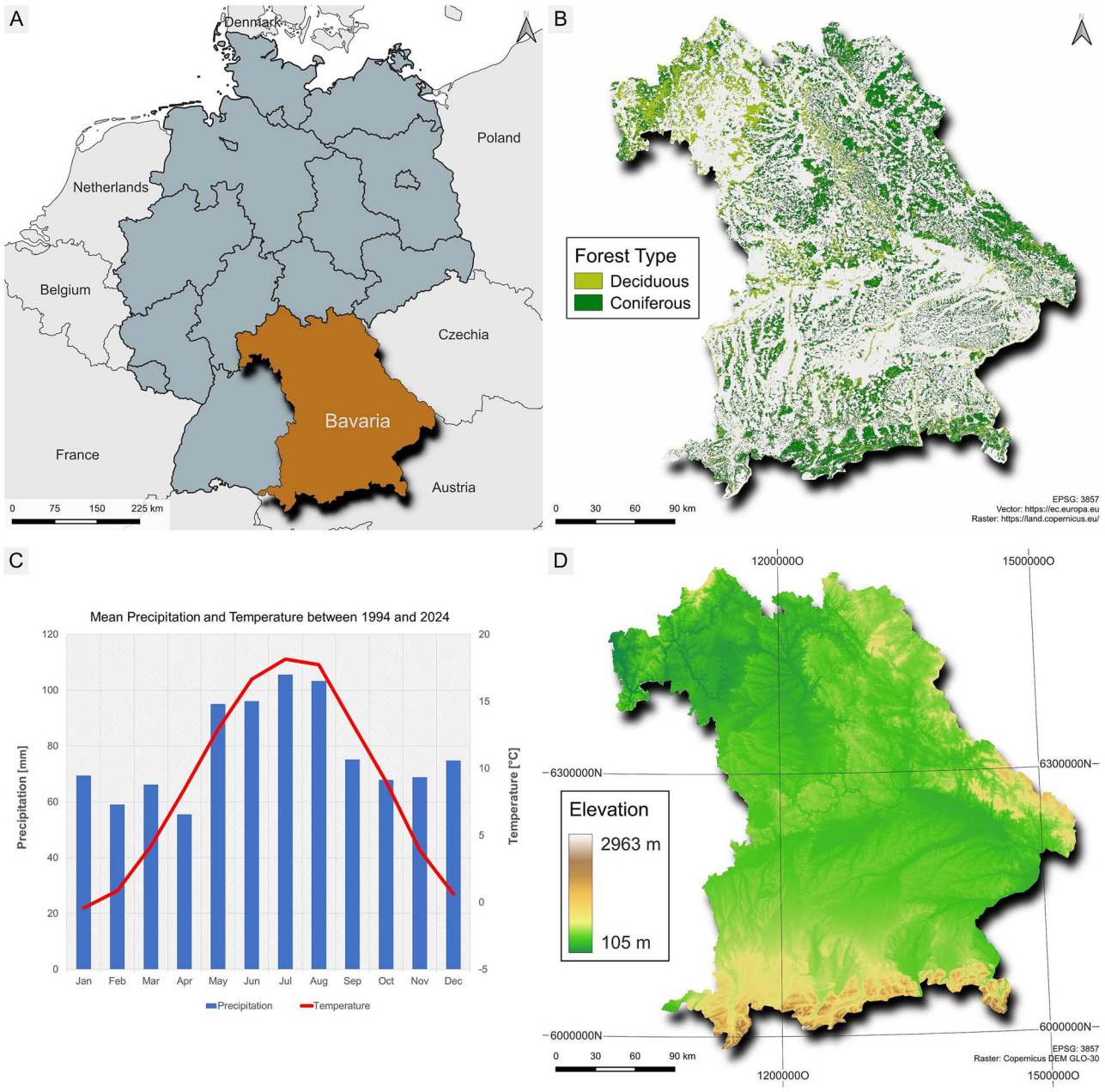

Figure 1 Bavaria is located in southeastern Germany (A). While the southern and eastern part is dominated by coniferous forests, the northwestern part shows a majority of deciduous forests (B). Bavaria is characterized by warm, wet summers and cold, dry winters (C). Elevation in Bavaria ranges from high mountainous alpine regions to hilly lowlands (D).

Ancillary data were used to produce a binary forest mask and corresponding forest type layer that separate areas into coniferous or deciduous forest. For the former, we chose the stocked forest area with a 10 m spatial resolution for the year 2018 (Langner *et al.*, 2022) as it is based on an enhanced forest definition for Germany, which defines forest as any area covered with forest plants (National Forest Inventory—Glossary). In addition, it includes any area that is permanently determined for production, including such cases of temporarily cleared spaces. We created the forest type layer using the Copernicus forest type layer from the Copernicus land monitoring service (CLMS) (European Environment Agency, 2020) and a tree species map for Germany (Blickensdörfer *et al.*, 2024) to fill in any gaps left where the CLMS forest type did not cover the stocked forest area. Because the CLMS and Blickensdörfer products do not completely cover the stocked forest layer, we only kept pixels in the forest mask for which we could retrieve the forest type. Since all three products share the reference year 2018, they are temporally well harmonized.

We applied a thorough preprocessing to the satellite data in order to reduce cloud-contamination and other possible artifacts such as cloud shadows in the time series to a minimum. After the initial cloud filtering (only scenes <80%), we used the scene classification layer provided with the data to mask out any presence of cloud shadows, different cloud types, nodata, or saturated areas. For the Landsat data, masking of low-quality data was performed using the quality bands

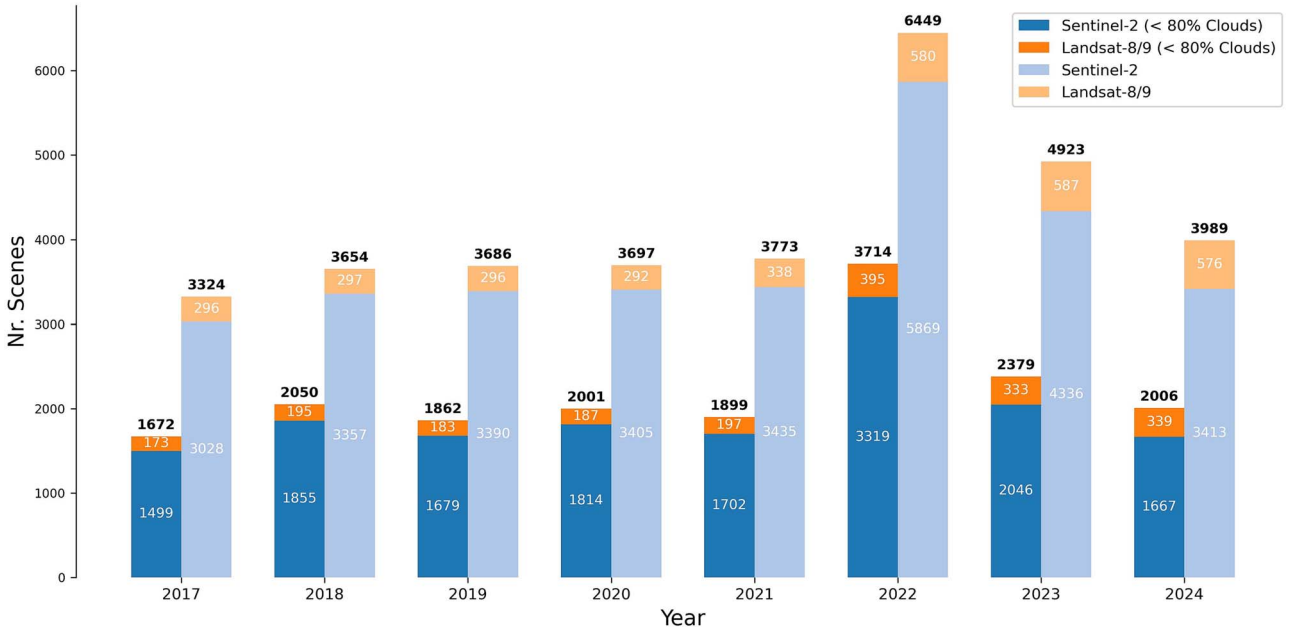

Figure 2 Scene counts for Bavaria for Sentinel-2 and Landsat-8/9 from 2017 to 2024. The darker colors show number of scenes with <80% cloud cover, and the lighter colors show all available scenes.

for saturation and pixel quality (Zhu *et al.*, 2015) to exclude saturated, cloudy, or cloud shadow pixels. In the following text, we applied the necessary scale and offset (0.0000275 and −0.2, respectively) to the Landsat data to derive physical reflectance units from the raw signed integer values, which are used for data storage. By clipping the data sets with our forest mask, we reduced the data volume as early as possible by limiting the processing to only forest-covered pixels. In order to work on a single dataset for the analysis, we stacked the bands from both satellite constellations. A further quality check was implemented by excluding scenes that contained only few valid pixels over forested areas, based on the assumption that these are leftovers of scenes heavily affected by clouds or other artifacts. To account for snow cover during the winter months, a combined snow mask using the normalized difference snow index (Riggs *et al.*, 1994) and S3 snow index (Shimamura *et al.*, 2006) was calculated and applied by thresholding both indices (NASA-DEVELOP, accessed 10 July 2024). This effectively removed snow-affected pixels from the dataset during winter, when there is usually extensive snow cover in Bavaria. To later calculate the disturbance index (DI), the first three tasseled cap (TC) components (Crist and Cicone, 1984), namely brightness, greenness, and wetness, were derived using the appropriate factors for surface reflectance data (Crist, 1985). These components are well known for highlighting relevant vegetation changes and are transformed as a linear combination into the DI to distinguish stand-replacing and non-stand-replacing forest disturbances from intact forest signatures (Healey *et al.* (2005), Hais *et al.* (2009)). However, before combining the components it was necessary to apply a re-scaling using the standard deviation and mean of forested pixels (Equation 1):

$$B_r = B - B_\mu/B_\sigma; \quad G_r = G - G_\mu/G_\sigma; \quad W_r = W - W_\mu/W_\sigma \qquad (1)$$

in which B_r, G_r, W_r correspond to the re-scaled Brightness, Greenness, and Wetness; B_μ, G_μ, W_μ to mean and B_σ, G_σ, W_σ to the standard deviation of the forest Brightness, Greenness, or Wetness components. The mean and standard deviation were derived by taking the regional forested areas from within a 35 x 35 km tile from the preprocessed dataset as reference samples to account for region-specific forest characteristics. Furthermore, the reference samples were split into a deciduous and coniferous reference using the aforementioned forest type mask. This forest-type-specific re-scaling accounts for seasonality. In a next step, the respective TC components were first transformed into separate deciduous and coniferous DI rasters (following Equation 2) and then combined to a single DI layer. The DI is defined as follows:

$$DI = B_r - (G_r + W_r) \qquad (2)$$

Despite the additional computational efforts required due to the re-scaling, the DI is well suited for this study because of its sensitivity toward forest disturbances and robustness against seasonality compared with other indices. Therefore, it was used in several studies to assess forest disturbances (Healey *et al.* (2005), Hais *et al.* (2009), Thonfeld *et al.* (2022)). While the DI of intact forests is usually below 0, disturbed forests show values considerably higher than 0. In the next step, we filtered the time series to retrieve a smooth signal and to reduce the impact of outliers. Therefore, time steps with no available data were filled by linear interpolation to allow the application of the Savitzky-Golay filter (Savitzky and Golay, 1964) with a window size of 30 observations. The filter works by fitting a low-degree polynomial in a moving window using a least squares approach. It is commonly applied where data need smoothing but important features are to be preserved. From the smoothed time series only the time steps where data were available before the interpolation were selected to not distort the signal by carrying artifacts. From there, the data are aggregated along the time axis as biweekly composites using the 10th percentile to further exclude possible high-valued outliers. The final processed time series is then stored on disk using the zarr format, which is optimized for chunked n-dimensional arrays, to allow easy

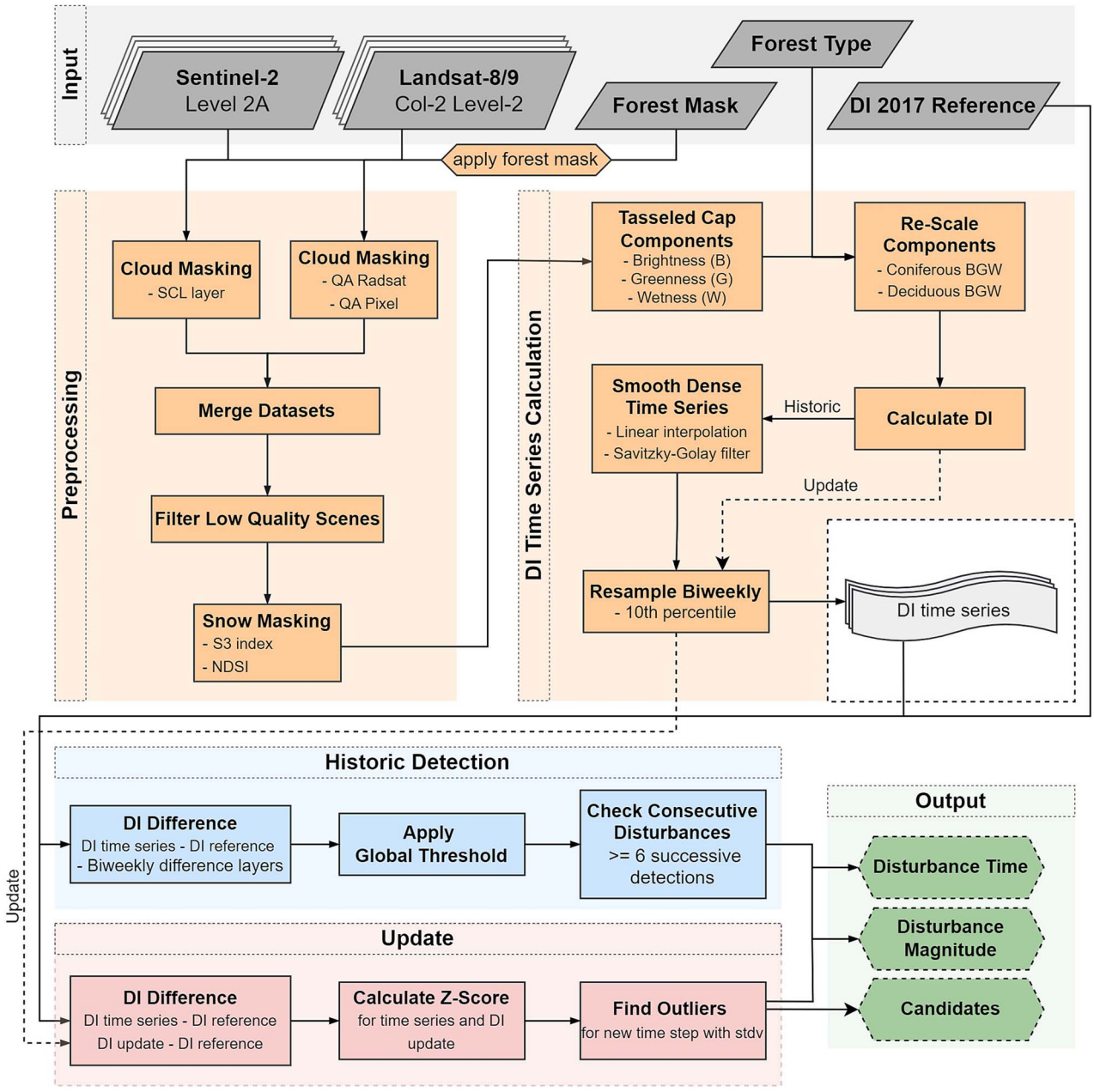

Figure 3 Workflow chart depicting all processing steps to calculate both past and recent forest canopy cover loss for entire Bavaria from 2017 to December 2024 at biweekly resolution using Sentinel-2 and Landsat-8/9 data. The core process (orange and blue/Preprocessing, DI Time Series Calculation, Historic Detection) follows Thonfeld *et al.* (2022) with some deviations and is extended by our NRT processing capabilities (orange and red/DI Time Series Calculation, Update). While the core process only returns the disturbance time and magnitude, the NRT approach additionally returns the candidate layer (green).

access for subsequent processing steps. An overview of our complete processing chain is shown in Fig. 3.

Time series change detection

Historic time series

The first part of implementing the monitoring system was the reconstruction of disturbances for previous years. We chose the year 2017 as reference because it represents the forests of Bavaria in a relatively vital state compared with the state after the following drought years from 2018 onwards (Senf and Seidl 2021a) and because the launch of Sentinel-2B increased data availability. The 2017 DI reference state was calculated by taking the pixel-wise median of all available Sentinel-2 and Landsat-8 scenes in that year. In order to retrieve biweekly difference images, we calculated the difference between the smoothed DI time series and the reference. On this dataset, we applied a global threshold of $th_{\Delta DI} \geq 3$. Although some variability in DI difference between regions can remain, we found that our threshold fulfills the necessary compromise for a cut-off value that balances the trade-off between true and false positive detections and captures the contrast between disturbed and undisturbed forest (Healey *et al.* (2005), Thonfeld *et al.* (2022)). Since the different forest types were

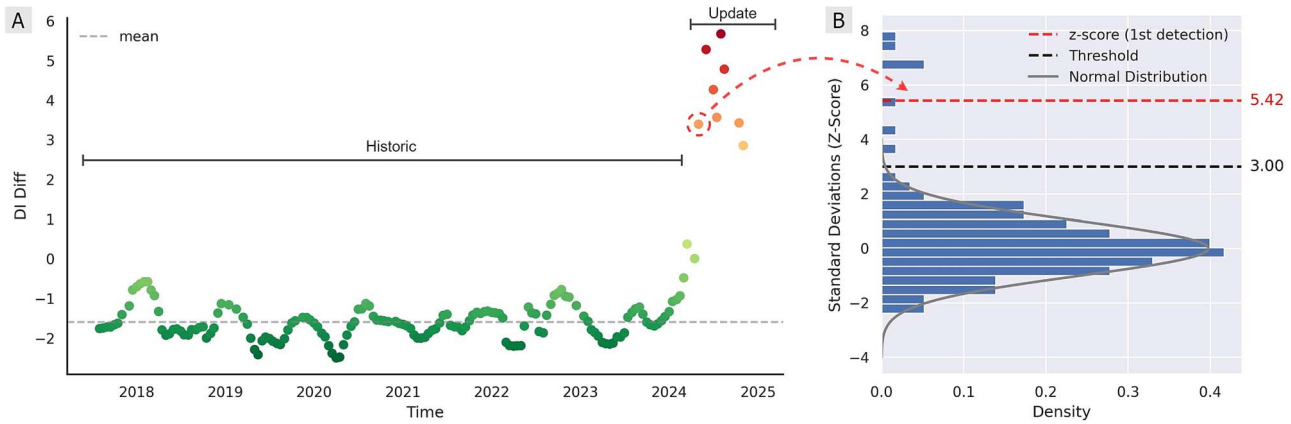

Figure 4 Depiction of how the NRT update works on an exemplary pixel in a spruce stand where trees were cleared and ground vegetation quickly regrew. Based on the historic time series (A), each subsequent time step is evaluated using the z-score of the past observations. When a deviation of $> 3\ \sigma$ is detected (B), the observation is logged as candidate. If the candidate is present in six consecutive observations it is considered a confirmed change.

already considered during index calculation, we applied the same threshold to the entire dataset. After thresholding, the resulting binary time series is used in subsequent steps to extract information about the disturbance time, disturbance magnitude, and to identify areas where consecutive changes occurred. To enhance the robustness of the disturbance detection we found that six consecutive changes, i.e. a time period of at least 3 months or more in the case of gaps in the time series, lead to accurate results. For a detected disturbance, the earliest time of change is logged as disturbance time. As additional information, we included the DI difference as disturbance magnitude.

Near real-time update

Building on the historic disturbance detection, we implemented the NRT monitoring mechanism from 1 April 2024 onward. One of the objectives was to move away from a fixed global threshold approach in favor of a data-driven method. We decided to analyze the DI difference in the historic time series to assess pixel-wise value distributions and the corresponding expected value ranges without an underlying theoretical model. This is common in other approaches to forest disturbance mapping (e.g. harmonic functions in Pasquarella *et al.* (2017); cosine and sine functions in Zhu and Woodcock (2014)). In other cases, such as the AVOCADO algorithm by Decuyper *et al.* (2022), the variability of seasonal phenology is considered. Since the DI levels out phenology and seasonal effects to a large extent, this was not relevant for us. The preprocessing of the new biweekly time step follows the methods described above but is extended by an additional intra-scene cloud masking to account for the missing Savitzky–Golay smoothing. The latter is omitted in the NRT update, since it requires a symmetric window around a data point, which is not given for the latest observation. Each scene within the new time step containing clouds is additionally processed, creating a mask using the 99th percentile of values in the blue band, efficiently masking effects such as cloud borders missed by the previously applied quality layers. After DI calculation and aggregation of scenes into a single raster, the new time step is appended to the stored time series to extend the continuous DI information. For finding the new disturbance candidates, we again calculated the DI difference to the state of the year 2017. However, instead of thresholding the difference image we calculated the z-score for each pixel using the historic time series, a measure also included in other NRT forest monitoring approaches (Pelletier *et al.*, 2024). Together with the pixel-based mean ($\mu_{(\text{hist})}$) and standard deviation ($\sigma_{(\text{hist})}$) from the historic DI difference, it is calculated as

$$z_{x,y} = \frac{x_{x,y} - \mu_{(\text{hist})x,y}}{\sigma_{(\text{hist})x,y}} \tag{3}$$

Because the z-score is a measure of how many standard deviations the new DI difference observation is from the historic mean, we had to define how many standard deviations we consider an outlier in the distribution and therefore a disturbance candidate. We found a value of $>$ 3SD to be accurate. Since these disturbances were detected only in a single time step, we did not consider them confirmed, but labeled them as candidates. To ensure the same robustness as for the historic detection, we created a corresponding candidate layer that keeps track of the candidate states for $x \in \{1, .., 6\}$ states, i.e. time steps. Again, only after six consecutive disturbances are changes considered confirmed, whereas the candidate state is reset to 0 as soon as a break is detected. The overview of the update stage is visualized in Fig. 4.

We additionally derived the distribution of canopy cover loss based on two different spatial features. On the one hand, we took a regular hexagonal grid, where each hexagon has an in-circle diameter of 20 km and covers 15 000 ha. We chose hexagons due to their advantages in representing curved features and gradual changes, equal size for direct feature comparison, reduced edge effects, as well as superior spatial relationship to neighboring hexagons compared with squares due to equidistant centroids (Birch *et al.*, 2007). On the other hand, we considered loss aggregated on the administrative level of districts (Landkreis).

Validation

In order to assess the accuracy of our disturbance maps, we followed the guidelines for land cover change accuracy assessment by Olofsson *et al.* (2014) and Stehman (2014). Therefore, we created the three strata undisturbed, disturbed, and buffer, based on the disturbances detected by our approach. This practice is referred to and used in comparable validation procedures (Olofsson *et al.* (2020), Francini *et al.* (2022), Thonfeld *et al.* (2022)). The buffer stratum is created by a 10 m inward and outward buffering of the disturbance areas.

Consequently, the disturbed stratum corresponds to the remaining disturbances, and the undisturbed stratum to the entire forested area outside the buffer stratum. Since uneven proportions of buffer and disturbed areas compared with the undisturbed areas would lead to only few validation points in the respective strata when applying the formula for random sampling by Olofsson *et al.* (2014), we resorted to the same solution as Reinosch *et al.* (2024) and randomly distributed at least 100 points in each stratum. We created a point validation set containing a total of 1042 samples, with at least 1 km distance between each point to avoid neighboring effects. We allocated 230 points in the buffer, 361 in the disturbed, and 451 in the undisturbed stratum. For each sample point, we visually checked whether any loss of canopy cover or dead trees was present using the digital orthoimagery at 0.2 m resolution provided by the Bavarian surveying administration (Orthophoto RGB 20cm, D, 2025) since 2006. However, the whole of Bavaria is only covered in a 3-year cycle until 2016 and a 2-year cycle since, which does not allow year-to-year comparisons. We decided to use reference imagery from before the start of our analysis in August 2017 coupled with the most recent available imagery for the respective area. Therefore, some sample points are validated up to including September 2023, while others reach into September 2024 (Fig. 5). Since recent imagery that covers the time of our NRT implementation is only available for half of Bavaria and with little temporal coverage of 3 to 6 months, only few validation points include the NRT method. The corresponding pre-disturbance reference imagery is either from 2015, 2016 or from the months in 2017 that are excluded in our analysis. Consequently, we focused the validation on the spatial accuracy of our maps, since the lack of temporally precise ground-truth data does not allow assessing temporal accuracy. The high spatial resolution of the reference data allows for a clear visual interpretation of canopy cover loss or dead trees in the case of the larger disturbances and in many cases where the resolution of Sentinel and Landsat data would be ambiguous. We labeled canopy cover loss if tree crowns showed strong signs of defoliation, were distinguishable as standing or lying deadwood, or were completely removed. To quantify the accuracy of our disturbance map, we calculated common accuracy metrics such as overall accuracy (OA), user accuracy (UA), producer accuracy (PA), and F1 score.

Results

Accuracy

The spatial accuracy assessment of our disturbance map shows an overall accuracy of 85.1±0.01% and an F1 score of 81% (Table 1). The user and producer accuracy for the disturbed class reached 73.9±0.01% and 89.7±0.01%, respectively. Regarding the sampling strata, we found the highest OA in the undisturbed stratum (96.5±0.0%), while we observed the lowest value in the buffer stratum with 74.8±0.03%. We also found differences between the strata for user and producer accuracy values. For the disturbed stratum, we achieved a UA of 78±0.02% for the canopy cover loss class, while in the buffer stratum an UA of 64±0.03% was observed. For the PA, again the buffer stratum showed a lower value of 78±0.03% compared with 97±0.01% for the disturbed stratum. Lastly, we again found this trend for the F1 score with 87% and 70% for the disturbed and buffer stratum, respectively.

The corresponding label distribution is shown in the confusion matrix in Table 2.

Forest canopy cover loss dynamics in Bavaria

For the final canopy cover loss detection, we evaluated the historic disturbance time series from August 2017 to the 1 April 2024 and then continued using the implemented update mechanism until including December 2024. We included the last months of 2017 to consider disturbances that occurred through summer storms in the same year. Our results reveal a total forest area of 160 921 ha, which shows canopy cover loss between August 2017 and December 2024 for entire Bavaria. This amounts to 6.5% of the forest cover of the entire state. These numbers include areas where dead trees have been removed and trees that have already died but remain as standing deadwood, since the DI is sensitive for both cases. We detected disturbances irrespective of the underlying drivers, including regular harvest. Concerning the annual development of the state forest canopy condition, the years 2019, 2020, and 2023 show exceptionally large-scale loss, with 28 867, 31 877, and 21 951 ha, respectively.

Spatially, we found that the entire forested landscape in Bavaria suffered from disturbances. However, specific hot-spot areas show consistently higher losses than others. Especially in northern Bavaria (Frankenwald in the district Kronach, (8245 ha, 22.2%)) on the Thuringian border and in eastern Bavaria (northern Bavarian Forest National Park in the Regen district (6195, 10.5%), district Passau (6855, 16.6%)) we observed large loss areas as well as high relative loss rates. Figure 6 provides a closer look at forest disturbances at state level, with local and regional examples from Steigerwald (A,D), the Frankenwald (B,E), and the Bavarian Forest National Park (C,F). These reveal both the spatial distribution, the time step, and the magnitude of the disturbances. The first panels (A, D) show an area in Steigerwald where the forest management practice of coppice with standards is practiced for successive years. Frankenwald, on the other hand, is marked by large-scale die-back of spruce stands, caused by combinations of drought and bark beetle infestations, that continuously increases through the years. The Bavarian Forest National Park shows fragmented loss patches in the unmanaged zones predominantly between the years 2018 and 2020 and from 2022 onward.

We calculated the absolute and relative loss for both types of aggregation features, hexagons, and Landkreise. Relative loss corresponds to the amount of disturbed area compared with the total forest area in the respective feature. The aggregated results in Fig. 7 show large-scale loss of canopy cover for districts in northern and eastern Bavaria, with Kronach and Passau showing 8245 and 6855 ha of disturbed forest per district between August 2017 and December 2024. While disturbances in the northeastern part are found mainly in coniferous forests, the situation in the western part is showing the opposite trend with large disturbance areas in deciduous stands. These disturbance patterns follow the underlying dominant tree types in the respective regions. The relative losses reveal that most districts experienced >5% canopy cover loss in forested areas within the last 7 years, with the exception of a few districts in southern and central Bavaria. Most districts with notably high absolute loss show equally high relative loss rates with >15% disturbed forest. Apart from the hot spots of disturbances that are coniferous-dominated districts, we observed no significant regional differences of relative loss rates between deciduous- and coniferous-dominated districts. The spatial distribution on the hexagonal level reveals that all of Bavaria is affected by canopy cover loss in absolute and relative terms. The largest absolute loss areas are observed for loss of coniferous forests

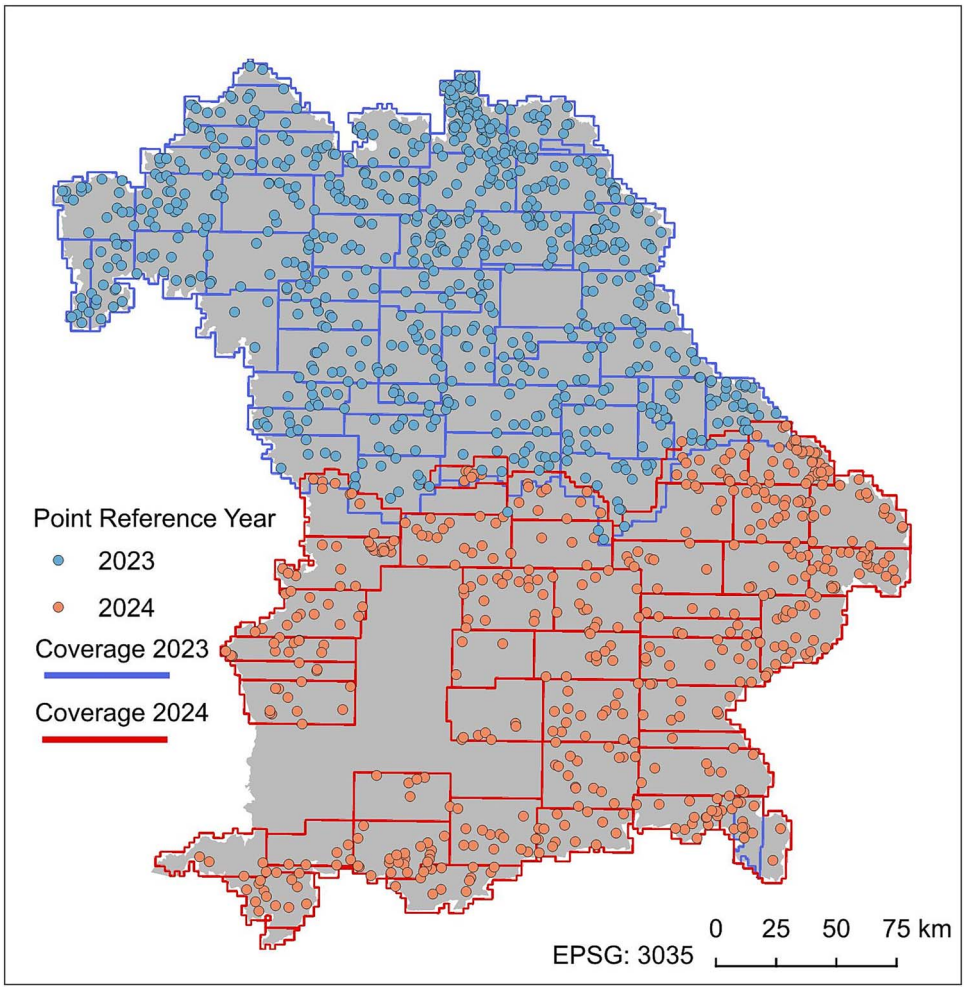

Figure 5 Spatial coverage of the most recent digital orthoimagery used for validating the disturbance map. Validation points (n= 1042) were randomly sampled in the strata disturbed, buffer and undisturbed.

Table 1 Results from the accuracy assessment reported across all sample strata and per stratum with respective standard errors. Whereas OA includes the canopy cover loss and the intact forest class, UA and PA values are calculated only for the canopy cover loss class.

	OA	OA±	PA	PA±	UA	UA±	F1
All strata	0.85	0.01	0.90	0.01	0.74	0.01	0.81
Disturbed stratum	0.78	0.02	0.97	0.01	0.78	0.02	0.87
Buffer stratum	0.75	0.03	0.78	0.03	0.64	0.03	0.70
Undisturbed stratum	0.97	0.00	-	-	-	-	-

Table 2 Confusion matrix for our validation process. Values ares summed across all strata.

		Prediction		
		Undisturbed	**Disturbed**	**Total**
Reference	Undisturbed	556	117	673
	Disturbed	38	331	369
	Total	594	448	1042

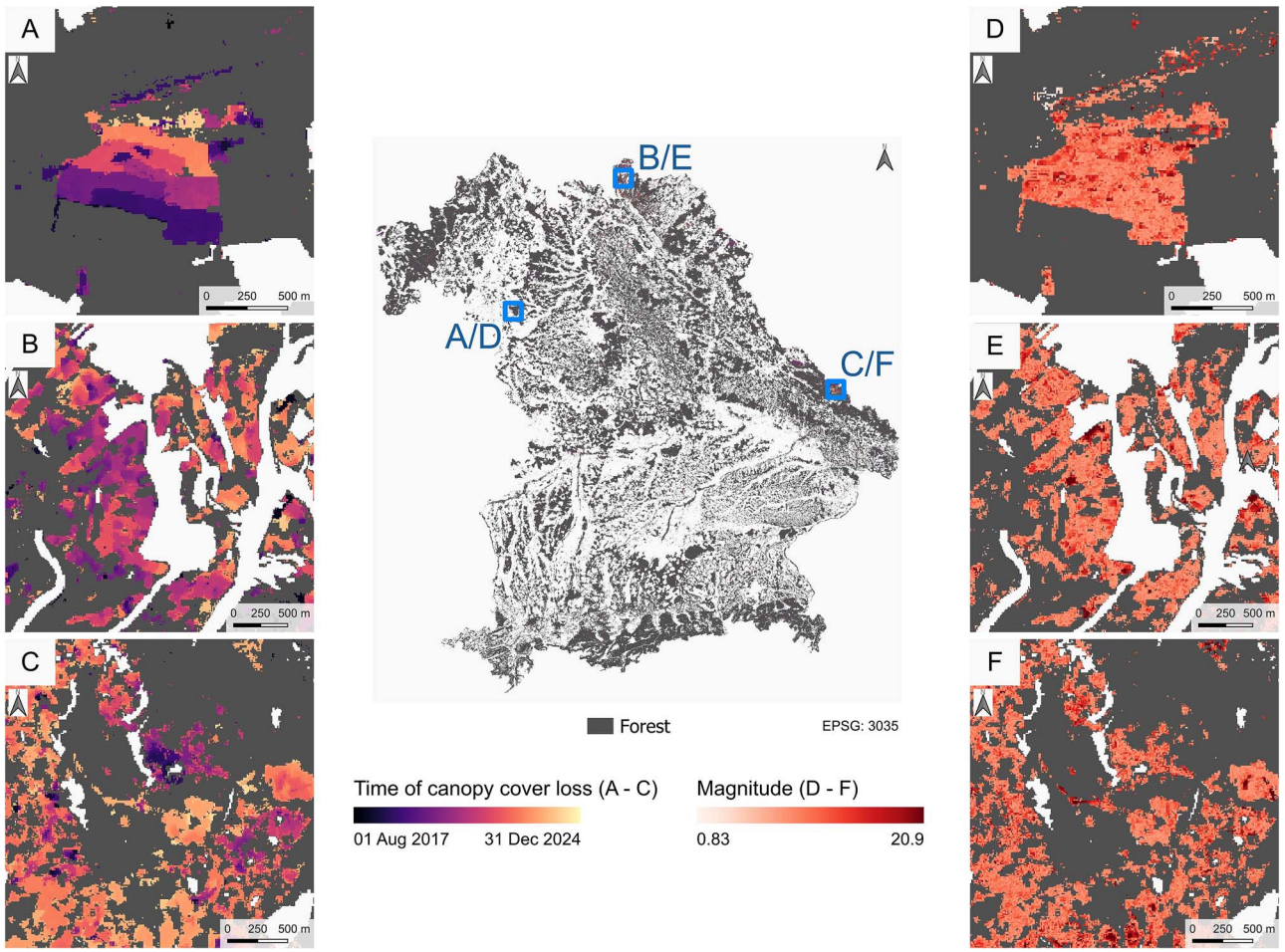

Figure 6 Biweekly canopy cover loss map and corresponding disturbance magnitude for entire Bavaria from August 2017 to December 2024. The selected regions of major forest disturbances are Steigerwald (A,D), Frankenwald (B,E), and the inner Bavarian Forest (C,F).

in northern and eastern Bavaria, although large areas of deciduous forests in northwestern Bavaria are also affected. The southern part of Bavaria shows less large-scale canopy cover loss with regional exceptions. However, the relative loss reveals that, although most of the alpine regions in the south remain less affected, the central lower regions from west to east generally lost 5%–10%, occasionally up to 20% of forested area (Fig. 7D).

The NRT detections account for 65.2% of canopy cover loss in 2024. Similar to the method employed for the historic detections, the NRT part manages to identify damages to the canopy cover, independent of the underlying driver. In northern Bavaria, the large-scale removal of spruce stands in spring is captured, whereas we observed regular forest harvest in the western region of Bavaria. As shown in Fig. 8, the mechanism allows for timely detection after the canopy is affected. In this case, management practices that are conducted regularly in the management zone of the Bavarian Forest National Park led to the removal of trees in the first half of July. In areas of regular cloud cover, the NRT method shows a tendency to detect more loss in the later months of the year compared with the retrospective method.

The NRT mechanism captures the tracking of consecutive candidate disturbances well (Fig. 9). This is important both for the reliable detection of consecutive disturbance events and to display the current status of newly detected disturbances. The resulting candidate maps therefore allow detailed insights for each possible disturbance pixel over the course of its confirmation.

Regarding the biweekly temporal resolution, we found areas throughout Bavaria (Fig. 10) where intra-month detections captured detailed canopy cover loss dynamics. Examples of this were found in coniferous as well as deciduous forests. Especially in larger forest patches that experience disturbances over several weeks helps our biweekly resolution in revealing the patterns of canopy cover loss.

Complementary to the time of disturbance, we also extracted the magnitude at the first point of detection in the time series. In our case, the magnitude corresponds to the DI difference of the biweekly mosaic and the 2017 reference. As shown in Fig. 11, diverging trends of magnitude values were found for the different management zones of the Bavarian Forest National Park. In both regional examples (B, C), notably higher values were present for disturbances that occurred in the management zone (yellow). This zone requires common management practices such as deadwood removal after bark beetle attacks to prevent spreading of infestations. In the core zone (green), the opposite was the case with largely lower magnitude values, separated sharply by the artificial administrative management border. Although higher magnitude patches were also found in the natural zone, the dominance of lower values is significant.

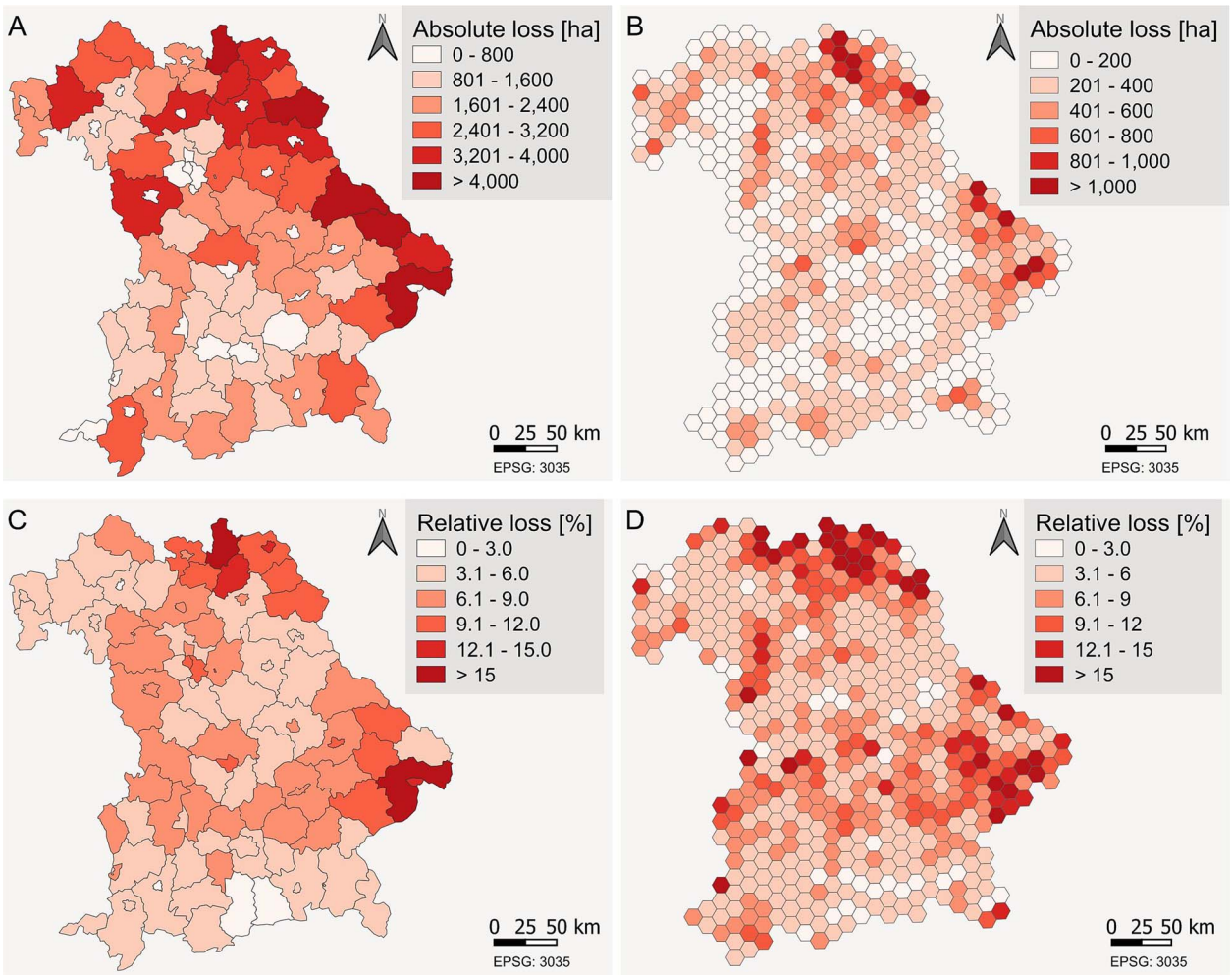

Figure 7 Comparison of absolute (A and B) and relative (C and D) canopy cover loss between administrative districts (Landkreise) (A and C) and a regular hexagonal grid (B and D) and from August 2017 to 2024. For each hexagon/district we calculated the relative loss by dividing the absolute forest by the total forest cover in the respective area.

Comparison with other products

A direct comparison of our canopy cover loss maps with results from other monitoring systems is in most cases difficult, due to the fact that each monitoring system has its own focus with corresponding assessment metric or specialized spectral index (e.g. DI for canopy cover loss, DWSI for forest vitality (LUP, 2024)). Therefore, we only conducted a quantitative comparison using the raw raster data with the annual forest disturbance maps by Hansen *et al.* (2013) as the data are publicly available. We observed that for all 6 years the total annual loss detected by us exceeds the disturbance area mapped by Hansen (Table 3). We attribute the large discrepancy in 2018 to larger patches of misclassifications in late autumn and early Winter 2018, where errors in the cloud masking layers led to spatially notable false positives. Effects like this contribute to our fairly high commission error. In 2019, we found that our maps exhibit much more small scale disturbances not captured by the Hansen product, leading again to large differences in annual disturbance area. While the remaining years (2018, 2021–2024) are well in agreement with the annual Hansen maps, we also found that within 2024, where we switched to the NRT method, we still detected a larger disturbance area. For the disturbed forest areas reported by NWA & RSS (2024) (Naturwald Akademie/Natural Forest Academy, Remote Sensing Solutions) we relied on the numbers reported in the online dashboard for Bavaria. Since the temporal resolutions differ significantly, we aggregated our results annually for all years where a full year was available (2018–2024). In comparison with the numbers from the Remote Sensing Solutions (RSS) map, we also find that for all years, our canopy cover loss areas are notably higher. Whereas the differences for the years 2019 and 2020 can be explained by the same reasons outlined above, another reason for the consistently lower numbers by RSS could be the minimum mapping unit of 0.03 ha. In a visual comparison of the web maps by RSS in hot spots of large-scale canopy cover loss, such as Franconia or the Bavarian National Park, we found that the results are well in agreement with our mapping, both spatially as well as for the year of disturbance.

Discussion

Near real-time updates of canopy cover loss

Our implementation of a biweekly canopy cover loss detection method demonstrates how NRT forest monitoring can be conducted for the entire German state of Bavaria using continuous data from two

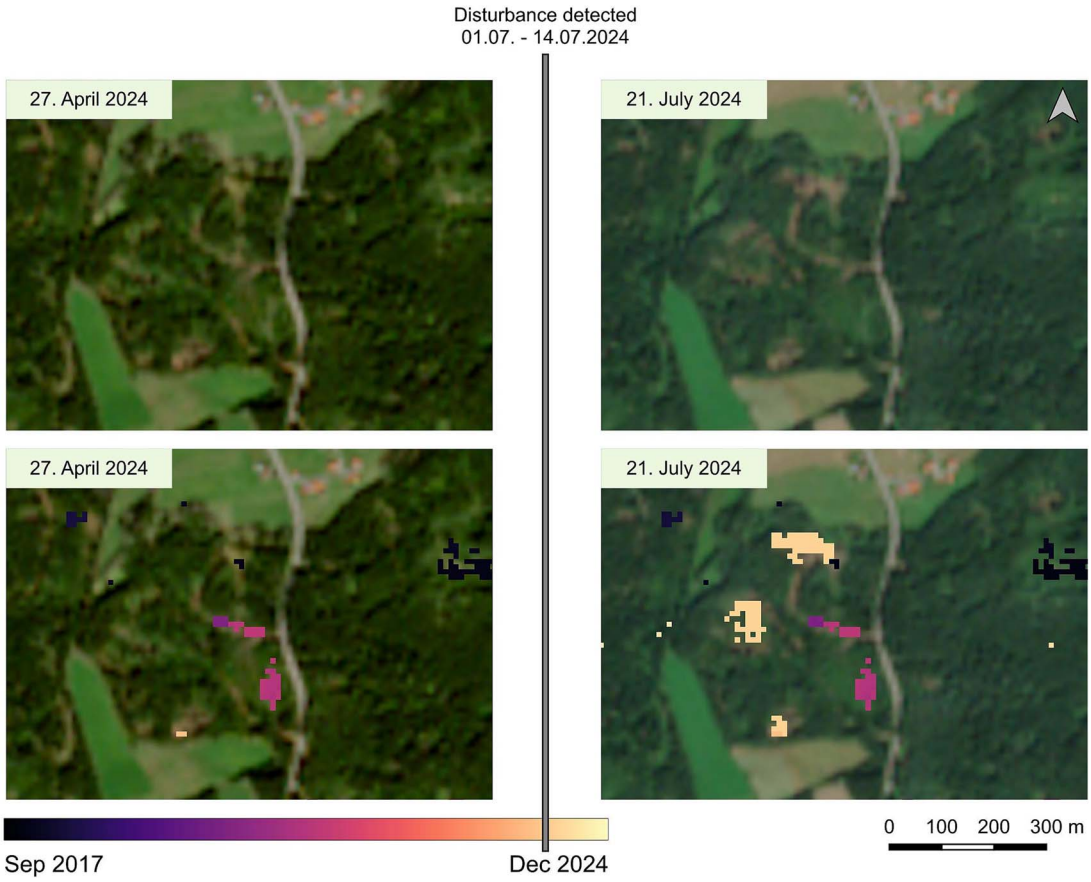

Figure 8 Example of canopy cover loss detected by the NRT mechanism in the first half of July 2024 in the Bavarian Forest National Park. The satellite imagery are Sentinel-2 acquisitions from the respective dates.

Table 3 Comparison of our results with the forest disturbance maps by Hansen *et al.* (2013) and NWA & RSS (2024). While our results and the values from the Hansen product are for the full respective year, RSS reports the values for the main vegetation period between 2 years. Therefore 2024 corresponds to forest disturbances between 2023 and 2024, while the early years are already aggregated from 2017 to 2020.

	Year						
	2018	**2019**	**2020**	**2021**	**2022**	**2023**	**2024**
Our results [ha]	17 310	28 867	31 877	18 329	16 944	21 951	16 007
Hansen et al. [ha]	13 463	14 846	19 198	17 249	12 075	23 067	10 484
RSS [ha]	22 583		7885	11 569	10 724	10 452	

multispectral satellite missions. The result is a monitoring system that provides year-round disturbance information at an update interval and spatial resolution currently not available in any other forest monitoring product and, therefore, allows unique insights into Bavarian forest disturbance dynamics. As described in Thonfeld *et al.* (2022), the core element for producing accurate forest disturbance maps is the implementation of mechanisms to control artifacts and outliers. Since faultless artifact filters are not available despite continuous improvements (e.g. Pasquarella *et al.* (2023)), the problem of outlier control in optical satellite imagery remains. Even in biweekly aggregated composites, undetected outliers can lead to values that misrepresent the current state at the ground and are therefore mistaken as disturbance. Consequently, it remains difficult to achieve highly accurate forest disturbance maps from only a few or single data points per pixel since higher temporal resolution (i.e. smaller aggregation units or time steps) leads to fewer available observations in a single step and consequently higher weights of single outliers. This persistent uncertainty in classifications demands to be communicated to map users to ensure trust in remote sensing products. We target outlier reduction by compositing multiple observations coupled with smoothing operations in pixel-based time series, hence reducing the impact of single observations and remaining artifacts. For the NRT processing, we provide a contextual information layer to the user through the candidate layer, which informs the user of the reliability of a respective disturbance. Currently, confirmation through consecutive observations remains a reliable choice for the robustness of the results (e.g. Zhu and Woodcock (2014), Reiche *et al.* (2021)). Regarding the temporal accuracy of detected disturbances, the accuracy of any NRT method heavily relies on data availability, which poses challenges for areas or time steps where limited data

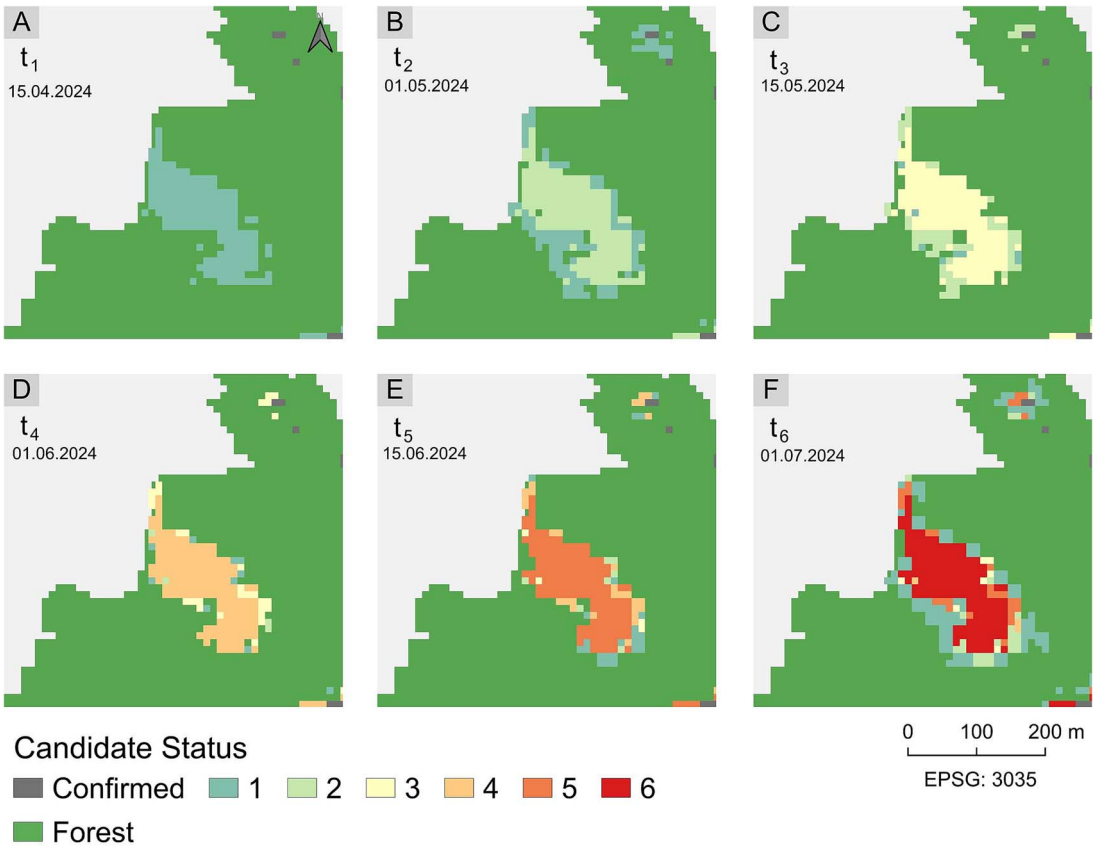

Figure 9 Evolution of candidate assignment over time. After six consecutively detected disturbances it is considered a robustly mapped loss of forest canopy cover. If the sequence of detections is interrupted by a valid observation not being identified as disturbance, the status is reset to 0.

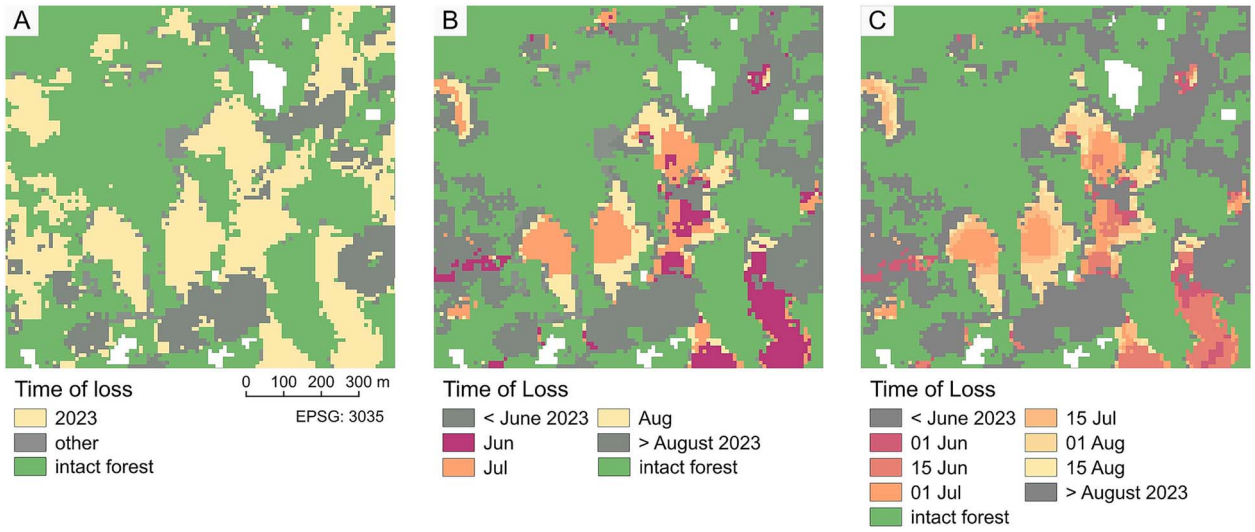

Figure 10 Comparison of how detected forest canopy cover loss differs for different temporal resolutions. Depicted are disturbances for the year 2023 (A), for the months of June, July, and August 2023 (B) and at intra-month resolution from June to August 2023 (C) for a disturbance patch in the Bavarian forest.

are available (Zhu, 2017). Consequently, we miss disturbances at times of unfavorable weather conditions (i.e. cloud cover) and in winter (i.e. under snow cover), which generally leads to a delay in the detection date. For approaches based on optical sensors such as ours, this limitation results in possible detection delays and requires careful evaluation of detections during the winter months. A general uncertainty is introduced by the occurrence of mixed forest stands. This class is not explicitly contained in our forest type layer

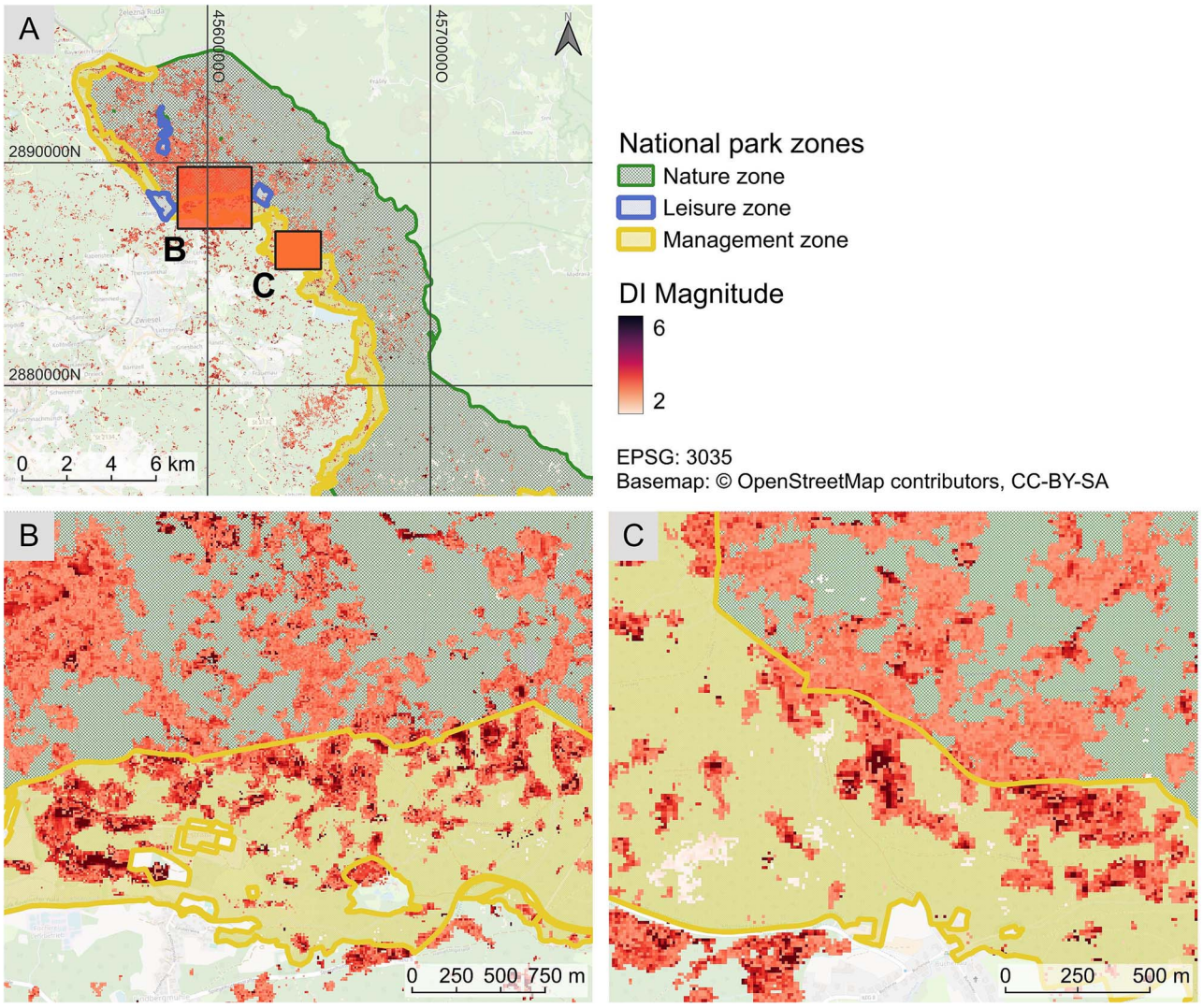

Figure 11 Spatial distribution of DI magnitude in the northern part of the Bavarian Forest National Park. The yellow/border zones correspond to management areas where actions such as salvage logging to restrict bark beetle infestations are taken. The green/inner zones are natural zones with no human interventions.

and therefore not considered in our analysis. In mixed stands, the influence of deciduous trees can possibly lead to an overestimation of canopy cover loss.

Regarding the selection of spectral indices for forest monitoring, many different single indices or combinations were considered in earlier studies. Among others, the most common include the NDVI (Marinelli *et al.* (2023), Lange *et al.* (2024)), enhanced vegetation index (Buras *et al.* (2020)), normalized burn ratio (Hermosilla *et al.* (2015), Marinelli *et al.* (2023)) and the normalized difference moisture index (Decuyper *et al.* (2022)). The DI provides several key advantages that made it our preferred index, such as its easy interpretability and stability regarding seasonality. Nevertheless, a potential variability is introduced through the dynamic nature of the reference or "re-scaling" population used to re-scale the Tasseled Cap indices for the DI transformation. However, the current re-scaling of TC values with regional information includes important regional context and extends an otherwise purely temporal pixel-based approach into the spatial domain. Additionally, the normalization of the DI per sensor facilitates the combination of the two different satellite missions (Sentinel-2 and Landsat).

Compared with other NRT algorithms, our approach has the advantage of simplicity regarding statistical modeling requirements and computational demands. Fitting a harmonic model (Fordead), initial model training (S-CCD), or automatically deriving stable periods (Bfast Monitor) requires careful fine-tuning. Especially when transferring methods to other settings (e.g. forest disturbances instead of general land cover change) or other regions, these models need to be retrained and refitted, while our approach should work out of the box for other temperate forests. Furthermore, we showed that observations from two different satellite constellations can be incorporated. This increases temporal coverage and the chance of higher quality composites compared with other NRT approaches tailored to single-sensor input. Currently, our method requires the calculation of the pixel-wise statistics for each new possible canopy cover loss detection. However, since these statistics are straightforward in how they are calculated, they are less computationally

demanding than re-fitting entire statistical models. This allows for efficient processing of large areas, which can be demanding for NRT methods. Bfast Monitor tackles this with heavy parallelization, but this process requires dedicated GPU resources (Gieseke *et al.*, 2020).

We observed the tendency of our approach to detect false positives in the autumn and winter months. We attribute this to issues with remaining artifacts due to the larger amount of cloud cover in these months. Additional uncertainties are introduced through the underlying dataset we included, such as the forest type layer. In areas where misclassifications of the forest type layer occur, the calculation of the DI includes the signal from coniferous and deciduous trees, increasing variability in the time series. This is particularly important with respect to seasonality, since the influence on the time series should be largely reduced in the normalization step, which is done separately for each forest type. Therefore, errors in the underlying tree types can propagate into the final DI signal. Both issues highlight the importance of thorough preprocessing as described by Thonfeld *et al.* (2022).

Concerning the comparison with other forest monitoring systems, certain constraints remain. For example, the forest condition monitor by Lange *et al.* (2024) produces monthly forest vitality information, but the declining forest vitality is not consistently linked to a distinct disturbance time. This prevents a systematic comparison of monthly results. At the time of writing, the product by Schiller *et al.* (2024) was not available to us. In addition, as it is available since June 2024, the total overlap only spans 6 months, which does not allow for a comprehensive comparison. Altogether, our biweekly disturbance monitoring integrates well with other forest monitoring efforts that cover Germany, including Bavaria. While some products provide information on forest vitality trends or change (Waldzustandsmonitor (Buras *et al.*, 2021), Forest Condition Monitor (Lange *et al.* (2024)), ForestWatch (LUP (2024)), Waldmonitor Deutschland (NWA & RSS (2024)) on varying combinations of spatial and temporal resolution and update cycles, the disturbance update mechanism presented here fills the gap regarding NRT information. Although methods with NRT capabilities in forest disturbance products have been developed for forests in other European regions (Mermoz *et al.* (2024): mainland France, Marinelli *et al.* (2023): northern Italy, Schiller *et al.* (2025): selected locations in Central Europe), such systems have their own monitoring focus (e.g. only clear cuts in France, early detection of bark beetle infestations in Central Europe) and currently do not provide data consistently covering Bavaria.

Robustness of canopy cover loss detection

Robust canopy cover loss assessment was achieved for the historic as well as the NRT detection. Whereas it was straightforward to detect consecutive disturbances in historic time series, the NRT update required ancillary information in the form of a candidate layer that tracks the amount of consecutive observations with every new incoming time step. Our results show that maintaining the mechanism of succeeding observations is indispensable for a realistic and reliable forest disturbance mapping. The amount of time steps necessary is thereby dependent on the respective length of the time step, as it determines the probability of high-quality input data. For our approach, the implemented six consecutive observations provided satisfying results, balancing the trade-off between eliminating temporary false detections and retaining the ability to detect disturbances at all. Particularly single scattered pixels that are classified within a single time step are effectively removed if they turn out to be false positives. In areas that are affected by regular cloud cover, this robustness requirement can lead to certain delays in the detection of disturbances. Regardless of when the sixth observation is reached, we always set the time step of the first observed disturbance as time of canopy cover loss. In general, the candidate layer successfully fulfills both the function for tracking disturbances in time as well as an uncertainty layer that supports interpretability for map viewers.

Biweekly resolution

The advantages of the higher temporal resolution differ for different temporal dynamics. For patches where the disturbance occurred within a single time step, the main benefit of the higher temporal resolution is the temporally more precise detection. For patches where disturbances occurred over several time steps, the higher temporal resolution allowed to capture the intra-month canopy cover loss dynamics well. Naturally, the decrease in length for the observation period down to two weeks resulted in smaller disturbance patches per time step, which can give a more fragmented impression. Therefore, the full benefit of intra-monthly forest dynamics was captured in areas with notable canopy cover loss of forest area across several consecutive weeks.

Disturbance magnitude

Since the DI magnitude values across all detected canopy cover loss pixels stretch across a certain range, these differences may possibly be linked to different types of disturbances. An area that is salvage logged after bark beetle infestations with minimal or no vegetation left is expected to yield higher magnitude values than trees that remain in place as standing deadwood or as a consequence of storm events in the form of lying deadwood. Our example in the Bavarian Forest National Park highlights the tendency of these differences between the respective management zones. However, properly investigating differences in disturbance magnitude between management zones requires detailed information on the exact cause and time of canopy cover loss, since only this information enables linking magnitude values to discrete disturbance events.

Implementation, further developments, and complementary products

The development of a production ready processing chain to continuously assess forest canopy cover loss in Bavaria constitutes only the first step in making forest disturbance information available to the general public. As a next step, it is necessary to connect the results from satellite image processing with other components. In our case, all relevant data products are connected to an experimental mobile app that will be soon publicly available in app stores. Having easy access through a low-barrier mobile map aims at facilitating user uptake of the disturbance product and satellite remote sensing technology in general, which demands clear communication of scientific results (Fassnacht *et al.*, 2023). Further developments aim to go beyond forest disturbance maps and magnitude to create complementary datasets that provide deeper insights into forest dynamics. This includes maps of deadwood occurrence in forests (status and type), which has a high relevance due to its ecological function regarding biodiversity (Müller *et al.*, 2018), and detailed disturbance driver attribution. Ideas

such as using advanced machine learning methods for the former are already being tested (Schiefer *et al.*, 2023) and existing work to build on for the latter is summarized in detail by Stahl *et al.* (2023). Complementary information on forest structure (Kacic *et al.*, 2023) would further extend our current canopy focused perspective on disturbance since the characterization of pre- and post-disturbance structures through various forest structure attributes (e.g. canopy height, total canopy cover, above-ground biomass density) enables a more thorough assessment of potential resilience against environmental pressure factors and habitat characteristics. Furthermore, combining remote sensing products with ecological *in situ* data would deepen the understanding of forest biodiversity dynamics. While it was shown how canopy openness affects insect diversity shortly after disturbance for several small disturbances in Central Europe (Kortmann *et al.*, 2026), large-scale assessments are missing. Fusing data collections from these two perspectives and extending it to entire regions, such as Bavaria, is a necessary step to progress from localized tree-focused assessments to a more comprehensive understanding of a forest ecosystem across space and time.

Conclusion

With this study, we present an NRT extension of a canopy cover loss detection approach that provides information at high spatial (10 m) and temporal (biweekly) resolution. For Bavaria, it is the first operational NRT method that shows seamless sub-monthly information on state-wide forest disturbances. While robust historic detections can be ensured through consecutive observations, our NRT approach emphasized the requirement of context in the form of a candidate layer that tracks the number of detections as a measure of uncertainty. In its current form, the method benefits from single-pixel statistics instead of complex model fitting, which significantly reduces computational demand. Although good results are achieved for distinctive canopy cover loss (e.g. clear-cuts), mixed pixels containing vital and disturbed canopy with ambiguous signal pose a challenge regarding robust detection. Additionally, our results are highly dependent on thorough preprocessing. Remaining artifacts, especially during autumn and winter months, increase commission errors. For Bavaria, we have found a continuously increasing canopy cover loss for the past 7 years with regional hot spots in regions dominated by spruce forests. Our method is developed to be a practical and efficient part of a processing pipeline that delivers timely information on recent forest disturbance events. While we focused on the temperate forests of Bavaria, Germany, the approach is generally transferable to other regions without the need for region-specific model training. However, regional forest characteristics that affect the time series still need careful consideration before transferring the method. Altogether, our canopy cover loss detection can support forest condition assessments and sustainable forest management practices with novel insights into forest dynamics. Together with complementary information, such as disturbance magnitude or forest structure, a deeper understanding of the characteristics and possibly the drivers of forest disturbances is possible.

Acknowledgements

This publication has been prepared using European Union's Copernicus Land Monitoring Service information; https://doi.org/10.2909/59b0620c-7bb4-4c82-b3ce-f16715573137

The authors gratefully acknowledge the computational and data resources provided through the joint high-performance data analytics (HPDA) project "terrabyte" of the German Aerospace Center (DLR) and the Leibniz Supercomputing Center (LRZ).

Author contributions

Niklas Jaggy (Conceptualization, Data curation, Formal analysis, Methodology, Software, Validation, Visualization, Writing—original draft, Writing—review & editing), Frank Thonfeld (Conceptualization, Funding acquisition, Methodology, Writing—review & editing), Patrick Kacic (Conceptualization, Writing—review & editing), Nikolas Herbst (Writing—review & editing), Mareike Kortmann (Writing—review & editing), Samuel Kounev (Writing—review & editing), Jörg Müller (Writing—review & editing), and Claudia Kuenzer (Conceptualization, Funding acquisition, Supervision, Writing—review & editing)

Supplementary material

Supplementary material is available at *Forestry: An International Journal Of Forest Research* online.

Declaration of competing interest

The authors declare that they have no known competing financial interests or personal relationships that could have appeared to influence the work reported in this paper.

Funding

This work was supported by the Bavarian Research Institute for Digital Transformation (bidt), an institute of the Bavarian Academy of Sciences and Humanities.

Data availability

The data underlying this article will be shared on reasonable request to the corresponding author.

References

Birch CP, Oom SP, Beecham JA. Rectangular and hexagonal grids used for observation, experiment and simulation in ecology. *Ecol Model* 2007;**206**:347–59. https://doi.org/10.1016/j.ecolmodel.2007.03.041.

Blickensdörfer L, Oehmichen K, Pflugmacher D. *et al.* National tree species mapping using Sentinel-1/2 time series and german national forest inventory data. *Remote Sens Environ* 2024;**304**:114069. https://doi.org/10.1016/j.rse.2024.114069.

BMEL. *Ergebnisse der Waldzustandserhebung 2024*, 2025. Bundesministerium für Landwirtschaft, Ernährung und Heimat, https://www.bmel.de/DE/themen/wald/wald-in-deutschland/waldzustandserhebung.html.

Bourgoin C, Ceccherini G, Girardello M. *et al.* Human degradation of tropical moist forests is greater than previously estimated. *Nature* 2024;**631**:570–6. https://doi.org/10.1038/s41586-024-07629-0.

Buras A, Rammig A, Zang CS. Quantifying impacts of the 2018 drought on European ecosystems in comparison to 2003. *Biogeosciences* 2020;**17**:1655–72. https://doi.org/10.5194/bg-17-1655-2020.

Buras A, Rammig A, Zang CS. The European forest condition monitor: using remotely sensed forest greenness to identify hot spots of forest decline. *Front Plant Sci* 2021;**12**:689220. https://doi.org/10.3389/fpls.2021.689220.

Carter S, Reiche J, Berkowitz P. *et al.* GFOI module: deforestation alerts. GFOI, 2024. https://www.reddcompass.org/mgd.

Coleman K, Müller J, Kuenzer C. Remote sensing of forests in Bavaria: a review. *Remote Sens* 2024;**16**:1805. https://doi.org/10.3390/rs16101805.

Coops NC, Tompalski P, Goodbody TRH. *et al.* Framework for near real-time forest inventory using multi source remote sensing data. *Forestry* 2022;**96**:1–19. https://doi.org/10.1093/forestry/cpac015.

Crawford CJ, Roy DP, Arab S. *et al.* The 50-year Landsat collection 2 archive. *Sci Remote Sensing* 2023;**8**:100103. https://doi.org/10.1016/j.srs.2023.100103.

Crist EP. A TM Tasseled Cap equivalent transformation for reflectance factor data. *Remote Sens Environ* 1985;**17**:301–6. https://doi.org/10.1016/0034-4257(85)90102-6.

Crist EP, Cicone RC. A physically-based transformation of thematic mapper data-the TM Tasseled Cap. *IEEE Trans Geosci Remote Sens* 1984;**GE-22**:256–63. https://doi.org/10.1109/tgrs.1984.350619.

de Brito MM. Compound and cascading drought impacts do not happen by chance: a proposal to quantify their relationships. *Sci Total Environ* 2021;**778**:146236. https://doi.org/10.1016/j.scitotenv.2021.146236.

Decuyper M, Chávez RO, Lohbeck M. *et al.* Continuous monitoring of forest change dynamics with satellite time series. *Remote Sens Environ* 2022;**269**:112829. https://doi.org/10.1016/j.rse.2021.112829.

Drusch M, del Bello U, Carlier S. *et al.* Sentinel-2: ESA's optical high-resolution mission for GMES operational services. *Remote Sens Environ* 2012;**120**:25–36. https://doi.org/10.1016/j.rse.2011.11.026.

Dutrieux R, Ose K, de Boissieu F. *et al.* fordead: a python package for vegetation anomalies detection from SENTINEL-2 images. 2024. Zenodo. https://doi.org/10.5281/zenodo.14053035.

Forest type 2018 (raster 10 m). 2020. Europe, 3-yearly, European Environment Agency. https://doi.org/10.2909/77873ff3-4edf-48d4-94cd-c5b7b61da29e

Fassnacht FE, White JC, Wulder MA. *et al.* Remote sensing in forestry: current challenges, considerations and directions. *Forestry* 2023;**97**:11–37. https://doi.org/10.1093/forestry/cpad024.

Francini S, McRoberts RE, D'Amico G. *et al.* An open science and open data approach for the statistically robust estimation of forest disturbance areas. *Int J Appl Earth Obs Geoinf* 2022;**106**:102663. https://doi.org/10.1016/j.jag.2021.102663.

Gieseke F, Rosca S, Henriksen T. *et al.* Massively-parallel change detection for satellite time series data with missing values. In: *2020 IEEE 36th International Conference on Data Engineering (ICDE)*. Dallas, TX, USA: IEEE, 2020, 385–96.

Haberstroh S, Werner C, Grün M. *et al.* Central European 2018 hot drought shifts scots pine forest to its tipping point. *Plant Biology* 2022;**24**:1186–97. https://doi.org/10.1111/plb.13455.

Hais M, Jonášová M, Langhammer J. *et al.* Comparison of two types of forest disturbance using multitemporal Landsat TM/ETM+ imagery and field vegetation data. *Remote Sens Environ* 2009;**113**:835–45. https://doi.org/10.1016/j.rse.2008.12.012.

Hansen MC, Krylov A, Tyukavina A. *et al.* Humid tropical forest disturbance alerts using Landsat data. *Environ Res Lett* 2016;**11**:034008. https://doi.org/10.1088/1748-9326/11/3/034008.

Hansen MC, Potapov PV, Moore R. *et al.* High-resolution global maps of 21st-century forest cover change. *Science* 2013;**342**:850–3. https://doi.org/10.1126/science.1244693.

Hartmann H, Bastos A, das AJ. *et al.* Climate change risks to global forest health: emergence of unexpected events of elevated tree mortality worldwide. *Annu Rev Plant Biol* 2022;**73**:673–702. https://doi.org/10.1146/annurev-arplant-102820-012804.

Healey S, Cohen W, Zhiqiang Y. *et al.* Comparison of tasseled cap-based Landsat data structures for use in forest disturbance detection. *Remote Sens Environ* 2005;**97**:301–10. https://doi.org/10.1016/j.rse.2005.05.009.

Hermosilla T, Wulder MA, White JC. *et al.* Regional detection, characterization, and attribution of annual forest change from 1984 to 2012 using Landsat-derived time-series metrics. *Remote Sens Environ* 2015;**170**:121–32. https://doi.org/10.1016/j.rse.2015.09.004.

Kacic P, Thonfeld F, Gessner U. *et al.* Forest structure characterization in Germany: novel products and analysis based on GEDI, Sentinel-1 and Sentinel-2 data. *Remote Sens* 2023;**15**:1969. https://doi.org/10.3390/rs15081969.

Knapp N, Wellbrock N, Bielefeldt J. *et al.* From single trees to country-wide maps: modeling mortality rates in Germany based on the crown condition survey. *For Ecol Manage* 2024;**568**:122081. https://doi.org/10.1016/j.foreco.2024.122081.

Kortmann M, Seidl R, Jaggy N. *et al.* The positive effects of canopy openness across post-disturbance management on insect diversity. *Biol Conserv* 2026;**313**:111647. https://doi.org/10.1016/j.biocon.2025.111647, https://www.sciencedirect.com/science/article/pii/S0006320725006846.

Lange M, Preidl S, Reichmuth A. *et al.* A continuous tree species-specific reflectance anomaly index reveals declining forest condition between 2016 and 2022 in Germany. *Remote Sens Environ* 2024;**312**:114323. https://doi.org/10.1016/j.rse.2024.114323.

Langner N, Oehmichen K, Henning L. *et al. Bestockte Holzbodenkarte*, Vol. **2018**, 2022. https://doi.org/10.3220/DATA20221205151218

LUP – Luftbild Umwelt Planung GmbH. *ForestWatch*, Potsdam, 2024. https://forestwatch.lup-umwelt.de/.

LWF. *Waldzustandserhebung*, 2023. https://www.lwf.bayern.de/forschungsfoerderung/348385/index.php. last accessed, 02.08.2024.

LWF. *Wald Im Wandel - Wald Und Forstwirtschat in BayernErgebnisse der Vierten Bundeswaldinventur*, Freising, 2024 https://www.lwf.bayern.de/mam/cms04/service/dateien/lwf_wald-im-wandel_barrierefrei.pdf.

Marinelli D, Dalponte M, Frizzera L. *et al.* A method for continuous sub-annual mapping of forest disturbances using optical time series. *Remote Sens Environ* 2023;**299**:113852. https://doi.org/10.1016/j.rse.2023.113852.

Mermoz S, Prieto JD, Planells M. *et al.* Sub-monthly assessment of temperate forest clear-cuts in mainland France. *IEEE J Sel Top Appl Earth Obs Remote Sens* 2024;**17**:1–24. https://doi.org/10.1109/jstars.2024.3429012.

Müller J, Noss RF, Thorn S. *et al.* Increasing disturbance demands new policies to conserve intact forest. *Conserv Lett* 2018;**12**:e12449. https://doi.org/10.1111/conl.12449.

Mullissa A, Saatchi S, Dalagnol R. *et al.* LUCA: a Sentinel-1 SAR-based global forest land use change alert. *Remote Sens* 2024;**16**:2151. https://doi.org/10.3390/rs16122151.

Mulverhill C, Coops NC, Achim A. Continuous monitoring and sub-annual change detection in high-latitude forests using harmonized Landsat Sentinel-2 data. *ISPRS J Photogramm Remote Sens* 2023;**197**:309–19. https://doi.org/10.1016/j.isprsjprs.2023.02.002.

NWA & RSS. *Waldmonitor Deutschland*, 2024 https://map3d.remote-sensing-solutions.de/waldmonitor-deutschland/static/media/FAQs_Waldzustand_062022.d67dbf74fb2dd9bce9e0.pdf.

Olofsson P, Arévalo P, Espejo AB. *et al.* Mitigating the effects of omission errors on area and area change estimates. *Remote Sens Environ* 2020;**236**:111492. https://doi.org/10.1016/j.rse.2019.111492.

Olofsson P, Foody GM, Herold M. *et al.* Good practices for estimating area and assessing accuracy of land change. *Remote Sens Environ* 2014;**148**:42–57. https://doi.org/10.1016/j.rse.2014.02.015.

Orthophoto RGB 20cm, D. *(DOP20 RGB): Bayerische Vermessungsverwaltung –www.geodaten.bayern.de (2025), Lizenz: CC BY 4.0*, Munich, 2025. https://geodatenonline.bayern.de/geodatenonline/seiten/wms_dop_hist, https://geodatenonline.bayern.de/geodatenonline/seiten/wms_dop_hist.

Pasquarella V, Bradley B, Woodcock C. Near-real-time monitoring of insect defoliation using Landsat time series. *Forests* 2017;**8**:275. https://doi.org/10.3390/f8080275.

Pasquarella VJ, Brown CF, Czerwinski W. *et al.* Comprehensive quality assessment of optical satellite imagery using weakly supervised video learning. In: *2023 IEEE/CVF Conference on Computer Vision and Pattern Recognition Workshops (CVPRW)*. Vancouver, BC, Canada: IEEE, 2023, 2125–35.

Patacca M, Lindner M, Lucas-Borja ME. *et al.* Significant increase in natural disturbance impacts on european forests since 1950. *Glob Chang Biol* 2022;**29**:1359–76. https://doi.org/10.1111/gcb.16531.

Pelletier F, Cardille JA, Wulder MA. *et al.* Inter- and intra-year forest change detection and monitoring of aboveground biomass dynamics using Sentinel-2 and Landsat. *Remote Sens Environ* 2024;**301**:113931. https://doi.org/10.1016/j.rse.2023.113931.

Pignatale FC. *Sen2Cor 2.11.00 Configuration and User Manual. OMPC. TPZG.SUM.001 1, ACRI-ST*, 2022. https://step.esa.int/thirdparties/sen2cor/2.11.0/docs/OMPC.TPZG.SUM.001\%20-\%20i1r0\%20-\%20Sen2Cor\%202.11.00\%20Configuration\%20and\%20User\%20Manual.pdf. last accessed, 02.08.2024.

Potocic N, Timmermann V, Ognjenovic M. *et al.* Tree health is deteriorating in the European forests. *Programme Co-ordinating Centre of ICP Forests, Thünen Institute of Forest Ecosystems* 2021. 5/2021. https://doi.org/10.3220/ICP1638780772000.

Rakovec O, Samaniego L, Hari V. *et al.* The 2018–2020 multi-year drought sets a new benchmark in Europe. *Earth's Future* 2022;**10**:e2021EF002394. https://doi.org/10.1029/2021ef002394.

Reiche J, Balling J, Pickens AH. *et al.* Integrating satellite-based forest disturbance alerts improves detection timeliness and confidence. *Environ Res Lett* 2024;**19**:054011. https://doi.org/10.1088/1748-9326/ad2d82.

Reiche J, Mullissa A, Slagter B. *et al.* Forest disturbance alerts for the Congo basin using Sentinel-1. *Environ Res Lett* 2021;**16**:024005. https://doi.org/10.1088/1748-9326/abd0a8.

Reinosch E, Backa J, Adler P. *et al.* Detailed validation of large-scale Sentinel-2-based forest disturbance maps across Germany. *Forestry* 2024;**98**:437–53. https://doi.org/10.1093/forestry/cpae038.

Riggs G, Hall D, Salomonson V. A snow index for the Landsat thematic mapper and moderate resolution imaging spectroradiometer. In: *Proceedings of IGARSS '94 - 1994 IEEE International Geoscience and Remote Sensing Symposium, volume 4 of IGARSS-94*. Pasadena, CA, USA: IEEE, 1994, 1942–4. https://doi.org/10.1109/IGARSS.1994.399618.

Roy D, Wulder MA, Loveland TR. *et al.* Landsat-8: science and product vision for terrestrial global change research. *Remote Sens Environ* 2014;**145**:154–72. https://doi.org/10.1016/j.rse.2014.02.001.

Savitzky A, Golay MJE. Smoothing and differentiation of data by simplified least squares procedures. *Anal Chem* 1964;**36**:1627–39. https://doi.org/10.1021/ac60214a047.

Schiefer F, Schmidtlein S, Frick A. *et al.* UAV-based reference data for the prediction of fractional cover of standing deadwood from Sentinel time series. *ISPRS Open J Photogramm Remote Sens* 2023;**8**:100034. https://doi.org/10.1016/j.ophoto.2023.100034.

Schiller C, Költzow J, Schwarz S. *et al.* Forest disturbance detection in Central Europe using transformers and Sentinel-2 time series. *Remote Sens Environ* 2024;**315**:114475. https://doi.org/10.1016/j.rse.2024.114475.

Schiller C, May J, Klinke R. *et al.* Early detection of bark beetle infestations in central Europe using deep learning–based reconstructions of irregular Sentinel-2 time series. *Forestry* 2025;cpaf053. https://doi.org/10.1093/forestry/cpaf053.

Senf C, Buras A, Zang CS. *et al.* Excess forest mortality is consistently linked to drought across Europe. *Nat Commun* 2020;**11**:6200. https://doi.org/10.1038/s41467-020-19924-1.

Senf C, Pflugmacher D, Zhiqiang Y. *et al.* Canopy mortality has doubled in Europe's temperate forests over the last three decades. *Nat Commun* 2018;**9**:4978. https://doi.org/10.1038/s41467-018-07539-6.

Senf C, Seidl R. Persistent impacts of the 2018 drought on forest disturbance regimes in europe. *Biogeosciences* 2021a;**18**:5223–30. https://doi.org/10.5194/bg-18-5223-2021.

Senf C, Seidl R. Storm and fire disturbances in Europe: distribution and trends. *Glob Chang Biol* 2021b;**27**:3605–19. https://doi.org/10.1111/gcb.15679.

Senf C, Seidl R, Hostert P. Remote sensing of forest insect disturbances: current state and future directions. *Int J Appl Earth Obs Geoinf* 2017;**60**:49–60. https://doi.org/10.1016/j.jag.2017.04.004.

Shang R, Zhu Z, Zhang J. *et al.* Near-real-time monitoring of land disturbance with harmonized Landsats 7–8 and Sentinel-2 data. *Remote Sens Environ* 2022;**278**:113073. https://doi.org/10.1016/j.rse.2022.113073.

Shimamura Y, Izumi T, Matsuyama H. Evaluation of a useful method to identify snow-covered areas under vegetation—comparisons among a newly proposed snow index, normalized difference snow index, and visible reflectance. *Int J Remote Sens* 2006;**27**:4867–84. https://doi.org/10.1080/01431160600639693.

Stahl AT, Andrus R, Hicke JA. *et al.* Automated attribution of forest disturbance types from remote sensing data: a synthesis. *Remote Sens Environ* 2023;**285**:113416. https://doi.org/10.1016/j.rse.2022.113416.

Statistisches Bundesamt (Destatis). *Timber Cutting According to Types of Timber by Länder*, 2024 Technical report. https://www.destatis.de/EN/Themes/Economic-Sectors-Enterprises/Agriculture-Forestry-Fisheries/Forestry-Wood/Tables/timber-cutting-according-to-types-of-timber.html. last accessed 21.10.2024

Stehman SV. Estimating area and map accuracy for stratified random sampling when the strata are different from the map classes. *Int J Remote Sens* 2014;**35**:4923–39. https://doi.org/10.1080/01431161.2014.930207.

Terrabyte. High-performance data analytics (hpda) project "terrabyte". 2024. https://docs.terrabyte.lrz.de/about/introduction/.

Thom D, Seidl R. Natural disturbance impacts on ecosystem services and biodiversity in temperate and boreal forests. *Biol Rev* 2015;**91**:760–81. https://doi.org/10.1111/brv.12193.

Thonfeld F, Gessner U, Holzwarth S. *et al.* A first assessment of canopy cover loss in Germany's forests after the 2018–2020 drought years. *Remote Sens* 2022;**14**:562. https://doi.org/10.3390/rs14030562.

Thonfeld F, Kacic P, Holzwarth S. *et al.* Forest canopy cover loss dynamics in Germany between 2017 and 2024: revealing regional differences. *Int J Appl Earth Obs Geoinf* 2026;**146**:105157. https://doi.org/10.1016/j.jag.2026.105157.

UFZ. *Forest Condition Monitor (Waldzustandsmonitor)*, 2024 last accessed: 27.07.2024 http://interaktiv.waldzustandsmonitor.de/.

Verbesselt J, Zeileis A, Herold M. Near real-time disturbance detection using satellite image time series. *Remote Sens Environ* 2012;**123**:98–108. https://doi.org/10.1016/j.rse.2012.02.022.

West E, Morley PJ, Jump AS. *et al.* Satellite data track spatial and temporal declines in European beech forest canopy characteristics associated with intense drought events in the rhön biosphere reserve, Central Germany. *Plant Biology* 2022;**24**:1120–31. https://doi.org/10.1111/plb.13391.

Wulder MA, Hermosilla T, Stinson G. *et al.* Satellite-based time series land cover and change information to map forest area consistent with national and international reporting requirements. *Forestry* 2020;**93**:331–43. https://doi.org/10.1093/forestry/cpaa006.

Ye S, Rogan J, Zhu Z. *et al.* A near-real-time approach for monitoring forest disturbance using Landsat time series: stochastic continuous change detection. *Remote Sens Environ* 2021;**252**:112167. https://doi.org/10.1016/j.rse.2020.112167.

Zhu Z. Change detection using Landsat time series: a review of frequencies, preprocessing, algorithms, and applications. *ISPRS J Photogramm Remote Sens* 2017;**130**:370–84. https://doi.org/10.1016/j.isprsjprs.2017.06.013.

Zhu Z, Wang S, Woodcock CE. Improvement and expansion of the Fmask algorithm: cloud, cloud shadow, and snow detection for Landsats 4–7, 8, and Sentinel 2 images. *Remote Sens Environ* 2015;**159**:269–77. https://doi.org/10.1016/j.rse.2014.12.014.

Zhu Z, Woodcock CE. Continuous change detection and classification of land cover using all available Landsat data. *Remote Sens Environ* 2014;**144**:152–71. https://doi.org/10.1016/j.rse.2014.01.011.

Zhu Z, Zhang J, Yang Z. *et al.* Continuous monitoring of land disturbance based on Landsat time series. *Remote Sens Environ* 2020;**238**:111116. https://doi.org/10.1016/j.rse.2019.03.009.

Forestry: An International Journal of Forest Research, 2026, **99**, cpag022
https://doi.org/10.1093/forestry/cpag022
Original Article